

Review

Not peer-reviewed version

A Comprehensive Review of Piezoelectric Ultrasonic Motors: Classifications, Characterization, Fabrication, Applications and Future Challenges

[Sidra Naz](#) and [Tian-Bing Xu](#) *

Posted Date: 3 September 2024

doi: 10.20944/preprints202408.2241.v1

Keywords: Piezoelectric; ultrasonic motors (USMs); traveling wave ultrasonic motor; standing wave ultrasonic motor; multi-DOF ultrasonic motors; fabrications; characterizations; applications; and challenges



Preprints.org is a free multidiscipline platform providing preprint service that is dedicated to making early versions of research outputs permanently available and citable. Preprints posted at Preprints.org appear in Web of Science, Crossref, Google Scholar, Scilit, Europe PMC.

Copyright: This is an open access article distributed under the Creative Commons Attribution License which permits unrestricted use, distribution, and reproduction in any medium, provided the original work is properly cited.

Review

Title: A comprehensive review of Piezoelectric Ultrasonic motors: Classifications, Characterization, Fabrication, Applications and Future Challenges

Sidra Naz ¹ and Tian-Bing Xu ^{2,*}

^{1,2} Department of Mechanical and Aerospace Engineering, Old Dominion University, Norfolk, VA, USA, 23529

* Correspondence: txxu@odu.edu;

Abstract: Piezoelectric ultrasonic motors (USMs) are actuators that use ultrasonic frequency piezoelectric vibration generated waves to transform electrical energy into rotary or translating motion. USMs are paid more attention because they offer distinct qualities over traditional magnet-coil-based motors, such as miniaturization, great accuracy, speed, non-magnetic nature, silent operation, straightforward construction, broad temperature operations, and adaptability. This review study focuses on the principle of USMs and their classifications, characterization, fabrication methods, applications, and future challenges. Firstly, the classifications of USMs, especially, standing wave, traveling wave, hybrid mode, multi degree of freedom USMs are summarized, and their respective functioning principles are explained. Secondly, the finite element modelling analysis for design and performance predictions, the conventional and nano/micro fabrication methods, and, the various characterization methods are presented. Thirdly, their advantages, such as high accuracy, small size, and silent operation and their benefits over conventional motors for the different specific applications are examined. In addition, the substantial contributions to a variety of technical fields like surgical robots, industrial, aerospace, and biomedical applications are introduced. Finally, their future prospects and challenges in USMs development, with an emphasis on downsizing, increasing efficiency, and new materials are outlined.

Keywords: Piezoelectric; ultrasonic motors (USMs); traveling wave ultrasonic motor; standing wave ultrasonic motor; multi-DOF ultrasonic motors; fabrications; characterizations; applications; and challenges

Introduction

Acoustic waves are an assortment of mechanical waves made up of mechanical vibration that is considered an immaculate and ecological energy source, is environmentally omnipresent[1,2,3,4]. The most tactical kind of sound wave among the many others, for instance infrasonic waves (below 20Hz), Human audible wave (20Hz-20,000Hz), and ultrasound (above 20,000Hz), is ultrasound [5,6]. Because of their elevated frequency and tiny wavelength, ultrasonic waves have the properties of vigorous directivity as well as a lengthy propagation distance, which have led to extensive research in detection and actuating generically in immense fields like surgery therapy[7,8], diagnostic imaging[9], food processing [10], degrade toxic compounds [11], welding and forming of metal and plastics [12], aerospace[13], robotics [14]etc.

Piezoelectric materials are the best at generating ultrasonic waves. Their distinguishing feature, the piezoelectric effect, transforms electrical to mechanical energy and vice versa, rendering them the backbone of the ultrasonic industry. They are capable of efficient energy transmission, allow for adjustable frequency ranges, have tiny and solid-state architecture, are robust, and are suitable for durable operation. These piezoelectric materials are used in electromechanical devices[15] such as transducers [16,17,18], sensors, and actuators[19,20]. These piezoelectric based devices are employed in wide applications including microphones[21], surface acoustic waves for space applications[22], accelerometers[23], pressure sensors[24], clocks and timing devices[25], traffics systems[26], non-destructive testing[27], Internet of things[28], under water SONAR [29,30], energy harvesting [31,32,33], medical applications [34,35] and many more. In ultrasonic based technology, piezoelectric

devices are irreplaceable for generating and receiving ultrasonic wave having high frequencies. Hence Piezoelectricity has a major impact on every aspect of our lives, from ordinary electronics in our wallets to complex gear in numerous sectors.

The origins of piezoelectric ultrasonic motors (USMs) can be traced back to the initial stages of investigating piezoelectric materials for use in motors. Figure 1 demonstrates a chronological sequence of significant milestones and achievements. The historical development of USMs demonstrates a persistent endeavor to utilize the capabilities of piezoelectric materials for effective and accurate motion control. From first theoretical notions to the implementation and extensive use by firms such as canon, USMs have emerged as valuable instruments in diverse fields[36,37].

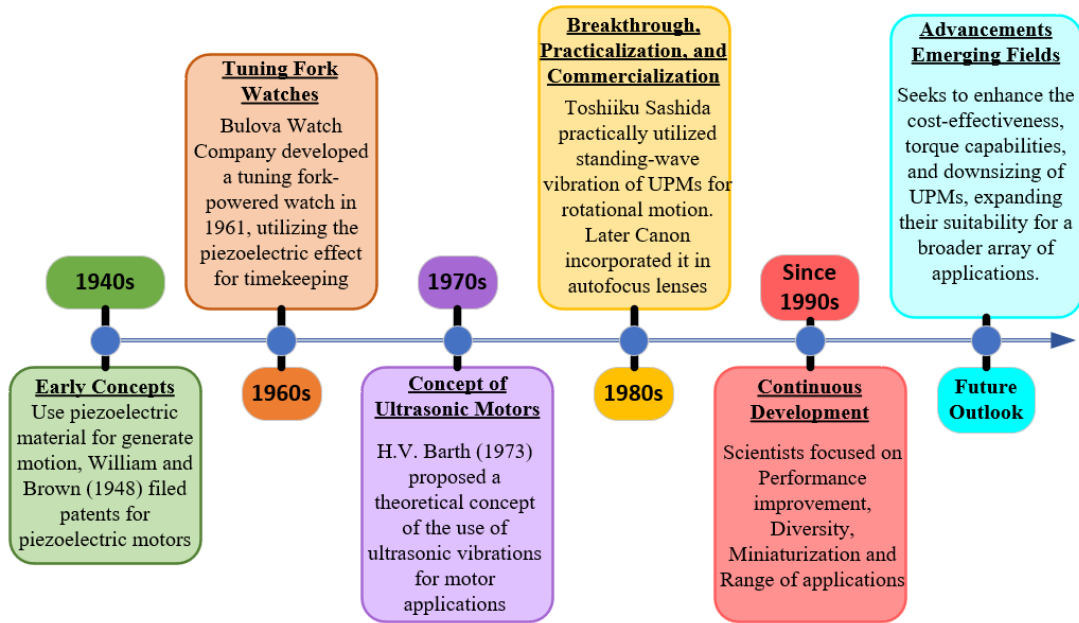


Figure 1. A chronological sequence of significant milestones and achievements of USMs.

1.1. Application of Piezoelectric Materials to USMs

Piezoelectric materials are essential to ultrasonic motor technology due to its ability to convert electrical energy into mechanical energy. They involve coupling of mechanical parameters (T , S) to electrical parameters (E , D) and forms electromechanical equations of piezoelectric elements. The direct piezoelectric effect is described in equation (1) while the inverse piezoelectric effect is described in equation (2).

$$D_m = d_{mj} T_j + \varepsilon_{mn}^T E_n \quad (m, n = 1, 2, 3) \quad (1)$$

$$S_i = s_{ij}^E T_j + d_{ni} E_n \quad (i, j = 1, 2, \dots, 6) \quad (2)$$

$$\begin{bmatrix} D_1 \\ D_2 \\ D_3 \end{bmatrix} = \begin{bmatrix} d_{11} & d_{12} & d_{13} & d_{14} & d_{15} & d_{16} \\ d_{21} & d_{22} & d_{23} & d_{24} & d_{25} & d_{26} \\ d_{31} & d_{32} & d_{33} & d_{34} & d_{35} & d_{36} \end{bmatrix} \begin{bmatrix} T_1 \\ T_2 \\ T_3 \\ T_4 \\ T_5 \\ T_6 \end{bmatrix} + 0; (E_n = 0) \quad (3)$$

$$\begin{bmatrix} S_1 \\ S_2 \\ S_3 \\ S_4 \\ S_5 \\ S_6 \end{bmatrix} = \begin{bmatrix} d_{11} & d_{21} & d_{31} \\ d_{12} & d_{22} & d_{32} \\ d_{13} & d_{23} & d_{33} \\ d_{14} & d_{24} & d_{34} \\ d_{15} & d_{25} & d_{35} \\ d_{16} & d_{26} & d_{36} \end{bmatrix} \begin{bmatrix} E_1 \\ E_2 \\ E_3 \end{bmatrix} + 0; (T_i = 0) \quad (4)$$

Where the symbol ϵ represents dielectric constant, D indicates electric displacement, E specify the electric field strength, d express piezoelectric constant, S denote the stress vector, s is the elastic compliance, and T represents the strain vector of piezoelectric material. Equation (3) represents the matrix form of coupling equation of direct piezoelectric effect, while equation (4) represents the matrix form of coupling equation of inverse piezoelectric effect. The mechanism of both direct and inverse piezoelectric effects is graphically shown in Figure 2. Where a generation of electric field in response of mechanical stress or external force is shown in Figure 2 (a) while the external electrical field applied to piezoelectrical material produce a structural deformation is shown in Figure 2(b). A symbol F indicates the applied force while E represents applied electric field.

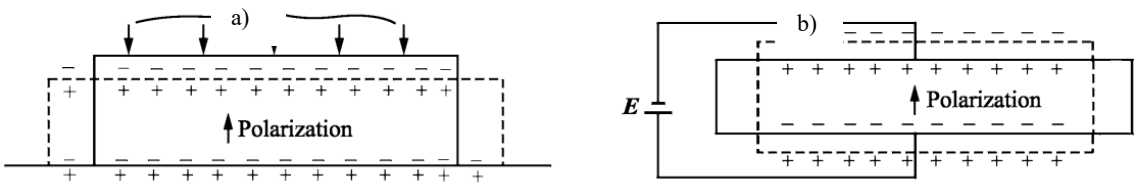


Figure 2. Polarization produces in Piezoelectric material: a) Direct piezoelectric effect, b) Converse piezoelectric effect.

Doping or swapping additives allows for a wide range of adjustments to the piezoelectric characteristics. The particular goals of the devices must be taken into consideration while determining the necessary characteristics of piezoelectric materials. For instance, the material must have a low permittivity and a modest high-frequency dielectric loss in order to be employed in high/ultra-high-frequency applications. The material's acoustic impedance and coupling coefficient are often put under strain in the context of energy transducer applications. A material that has great frequency stability and high mechanical quality factor (Q_m) values can be used as standard frequency oscillators. To meet the requirements of the delay line application, the materials must be frequency stable, and the sound velocity in materials must also be taken into account. Ceramics employed in the electro-acoustic area must possess a significant permittivity, electromechanical coupling factor k_p value, and elastic compliance coefficient however, dielectric loss have little effect on the devices. For hydroacoustic transducer applications, if employed as receivers, the material must have high k_p value, a big piezoelectric coefficient of g_{33} or g_{31} , and compliance constant, with a large permittivity, however its Q_m value is not strictly required. On the other hand, if piezoelectric material is used as a power emitter in hydroacoustic transducers, it is necessary that it has a little dielectric loss ($\tan\theta$), a high dielectric constant, great Q_m under a range of electric field, large piezoelectric constant, and high k_p value. Filters require materials that possess exceptional durability and resistance to temperature fluctuations. Additionally, these materials should exhibit high Q_m and low $\tan\theta$. The specific value of k_p needed for the filters depends on their bandwidth. High-voltage generators and igniters necessitate materials with high values of g_{33} and k_{33} , a high permittivity, a high Q_m , and a low $\tan\theta$. Hence USMs are highly dependent on the characteristics of the piezoelectric materials that are employed in their fabrication. Table 1 shows a list of commonly used piezoelectric materials in ultrasonic motor, including their most notable characteristics, advantages and disadvantages. In modern times, the properties of piezoelectric ceramics may be finely tuned throughout a broad spectrum through the use of doping and substitution techniques, allowing them to be tailored for many application scenarios [38,39,40].

Table 1. A list of commonly used piezoelectric materials in USMs, including their characteristics, advantages, and disadvantages.

Material	Characteristics	Advantages	Disadvantages
----------	-----------------	------------	---------------

Lead Zirconate Titanate (PZT)	<ul style="list-style-type: none">➤ Most common material➤ High piezoelectric coefficient➤ Tailorable properties	<ul style="list-style-type: none">➤ Widely available➤ High efficiency	<ul style="list-style-type: none">➤ Aging effects➤ Lead content (environmental concerns)
Single Crystal Piezoelectric Materials (e.g., Lithium Niobate)	<ul style="list-style-type: none">➤ Excellent mechanical properties➤ Exceptional piezoelectric coefficients	<ul style="list-style-type: none">➤ Superior strength and wear resistance➤ High performance	<ul style="list-style-type: none">➤ High cost➤ Less scalable➤ Manufacturing challenges
Lead-Free Piezoelectric Ceramics	<ul style="list-style-type: none">➤ Potential for higher operating temperatures➤ Environmentally friendly alternative	<ul style="list-style-type: none">➤ Reduced environmental impact	<ul style="list-style-type: none">➤ Lower efficiency➤ Lower piezoelectric coefficients➤ Limited availability (more expensive)
Piezoelectric Polymers (e.g., PVDF)	<ul style="list-style-type: none">➤ Lightweight and flexible➤ Low cost	<ul style="list-style-type: none">➤ Design advantages for compact USMs➤ Potentially cost-effective	<ul style="list-style-type: none">➤ Lower efficiency➤ Lower piezoelectric coefficients➤ Limited temperature range

1.2. Piezoelectric USMs:

Piezoelectric USMs leverage the inverse piezoelectric effect and the frictional coupling to transform electric inputs to mechanical outcomes. Based on their vibration states, they can be classed as resonant and non-resonant. Non-resonant piezoelectric motors often achieve efficiencies near the nanoscale magnitude; however, their highest velocity is barely tens of millimeters/second [41,42]. Resonant piezoelectric motors achieve significantly greater velocities and exceeding one meter/second [43,44,45,46,47,48]. The resonant piezoelectric motor can be referred to as piezoelectric ultrasonic motors (USMs) because it operates at a frequency that is usually greater than 20kHz to prevent damaging individual hearing. As a solid-state actuator, the USMs offers advantages over electrostatic motors, electromagnetic motors, electro-conjugate fluid motors, and thermal mechanical motors in terms of simplicity of design, rapid response, a substantial output torque at a small size, and freedom from electromagnetic interference [49,50,51]. In the previous decade, several unique USMs have been suggested to implemented in many fields such as invasive surgical procedures, handling medications, optical focusing systems, microrobots, and aeronautical devices.

Table 2. Advantages of piezoelectric USMs over other traditional motors.

Feature	Piezoelectric Ultrasonic Motor	Electromagnetic Motor	Electrostatic Motor	Thermal Mechanical Motor	Electro-Conjugate Fluid Motor
Voltage(I/P)	Lower voltage	Lower voltage	High voltage required	Moderate voltage	Moderate voltage

Size & Weight	Compact and lightweight	Bulky due to magnets and coils	Can be bulky and heavy	Can be bulky	Can be complex
Suitable Environment	Works in air and vacuum	Affected by magnetic fields	Limited by air breakdown	Sensitive to temperature	Sensitive to leaks
Noise	Silent operation	Can be noisy (brushes/gears)	May generate noise	May generate noise	May generate noise
Electromagnetic Interference (EMI)	No EMI	Generates EMI	May generate EMI	No EMI	No EMI
Low-Speed Torque	High torque at low speeds	Torque decreases at low speeds	Limited torque at low speeds	Limited torque at low speeds	Generally lower torque
Response Time	Very fast response time	Can be slow depending on design	Slower response time	Slowest response time	Slower response time
Motor Complexity	Simple design	Complex design with moving parts	Complex design	Complex heating/cooling system	Complex fluid dynamics
Temperature	Stable performance across a wide range	Performance may be affected	Performance may be affected	Performance may be affected	Performance may be affected
Motor Efficiency	High efficiency, especially at low speeds	Varies depending on design	Lower efficiency	Lower efficiency	Lower efficiency

1.3. Basic Operating principle of USMs:

Ultrasonic piezoelectric motor is comprised of two primary components: stator and rotor. The stator is the immobile part that contains the piezoelectric components. The stator design can change based on the exact type of ultrasonic motor such as standing wave or traveling wave. While the rotor is the mobile part that works with the stator to produce rotational or linear movement[52]. The USMs universal working concept is to convert the spiraling driving foot motion to the movement of the rotor via the friction interaction that occurs between the rotor and its stator, demonstrated in figure 3. The pushing element of the circular motion moves the runner with the friction force, while the pressing element shifts the force that are normal within the driving foot and the runner on a periodic basis. The pushing and pressing elements are parallel and perpendicular to the runner's traveling trajectory respectively. In figure 3, from point P to Q, the normal and frictional forces increase, and driving foot's horizontal speed exceeds the runner speed causing the driving foot accelerates the runner. The normal force drops in the direction Q to R, and the flow of friction force drive backwards, and driving foot's horizontal speed falls than the runner speed. As a result, driving foot accelerate down the runner. The friction and normal forces rise from R to P, where the runner's speed decreases further. Hence in this manner, the circular motion behavior of driving foot causes to move the runner

periodically. Therefore, the pressing and pushing elements of the circular movements have the predominant impact on the motor's thrust and speed, respectively[53].

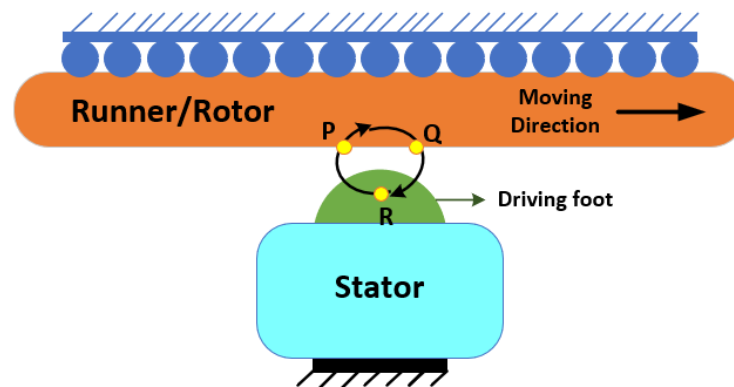


Figure 3. Basic operation of USM.

1.4. Characteristics of USMs:

Advantages

- USMs have the benefits of nano/micro-structure and allows variety of flexible designs. Because of the piezoelectric material characteristic that can produce many forms of vibration, involving bending, longitudinal, and torsional vibrations. The torque density of USMs is greater than conventional motors.
- USMs provide strong torque at low speeds and are capable of driving loads directly with no gear requirement. This advantage improves positioning accuracy as well as response speed by reducing additional weight and volume imposed by the gearbox, transmission-induced position error, vibrations, noise, and energy loss.
- USM's rotor possesses tiny inertia, rapid response at the microsecond level, self-locking, and high holding torque. They may reach a stable speed in a few milliseconds and stop even faster due to friction between the rotor and stator.
- The Position and velocity control of USMs is great with good displacement resolution. Because the stator operates at a high frequency and the rotor or slider is at low frequency. They are capable of controlling precision of microns or even nanoseconds in a servo system and hence responds quickly.
- USMs have distinct characteristics from regular motors as they generate no magnetic fields and are resistant to electromagnetic interference when operating.
- They are environmentally friendly devices due to low noise. USMs typically operate at frequencies greater than 20kHz, which are beyond human hearing. Furthermore, the noise generated by the gearbox to decrease the speed is eliminated because the motor can directly drive loads.
- USMs can operate under harsh environmental circumstances may be in vacuum and high/low temperature with selecting proper design, fractional part, and piezoelectric material.

Disadvantages

- USMs usually generate small power with low efficiency as they involve two step energy conversion techniques. The first approach uses the reverse piezoelectric effect to transform electrical power into mechanical energy. The second mechanism converts the stator's vibration into macro one-directional motion of the rotor via friction between its rotor and stator, which cause energy loss. Hence the overall effectiveness of USMs is reduced.
- It has a limited functional life and is not appropriate for continuous operation for long period. Friction and wear issues emerge at the stator-rotor interfaces during friction drive. Furthermore, high-frequency vibration can cause fatigue damage to the rotor and piezoelectric materials,

particularly when the power output is large and the ambient temperature is high which cause reduced the performance.

- The USMs have specific criteria of excitation/drive signals for the amplitude, frequency, and phase in order to activate the stator's resonance. Whenever the motor temperature varies, the frequency of excitation signals for piezoelectric devices must be adjusted appropriately to ensure output performance stability. Thus, the circuitry for USMs drivers is sophisticated as well.

1.5. Organization

In this paper, the operational principles, characteristics of various classifications, state of the art designs, their finite element modeling, fabrication, characterizations, application in different fields, challenges, and future trends of USMs are investigated in detailed. This paper is organized as follows: Section 2 discuss the classification of USMs including traveling wave, standing wave, hybrid mode, multiple degree of freedom USMs and their performances analysis. Section 3 shade light on the 3D finite element modeling of USMs. Section 4 describe the various types of existing fabrication methods that includes conventional and micro/nano fabrication methods of USMs. The performance, material, and dynamic characterization of USMs are elaborated in section 5. Furthermore, section 6 provide discussion of USMs in various applications like surgical robots, industrial, aerospace, and biomedical fields. Section 7 reports some trends and future challenges of USMs and section 8 provide the summary of the paper achievements and contributions.

Classification of USMs

The USMs principally divides into three categories: the standing wave USMs (SUSMs)[54,55,56,57,58] the traveling wave ultrasonic piezoelectric motor (TUSMs)[59,60,61,62,63,64,65,66], and the hybrid modes ultrasonic piezoelectric motor (HUSMs) [67] based on the technique in which the driving foot acquiring circular movement. The divisions of the USMs are graphically illustrated in figure 4. The TUSMs produces elliptical moment via creating a traveling wave within the stator, which is further classified into more three categories based on the mode of stator's vibration that are a disk's axial bending mode, a cylinder's radial mode, and a ring's axial bending mode. The SUSMs produces elliptical movements by triggering the stator's standing wave, and many vibration modes are applied. SUSMs are characterized as unidirectional or bidirectional motors based on the runner's output movements rather than the stator's vibration patterns[68,69,70,71]. The circular movement of HUSMs is achieved by creating two distinct modes of vibration for identical frequency and are divided in four categories based on the stator's vibrations. These classifications include longitudinal- longitudinal, bending-bending, longitudinal-torsional and longitudinal-bending categories. USMs can also be classified as single-degree-of-freedom (S-DOF), and multi-degree-of-freedom (M-DOF) motors based on their output movements. S-DOF motion that includes linear and rotational motion is possible with any working fundamental of the TUSMs, SUSMs, or HUSMs. The USMs provides a versatile technique to produce M-DOF movements, as the operational principles of the TUSMs, SUSMs, and HUSMs may be applied in USMs independently or together.

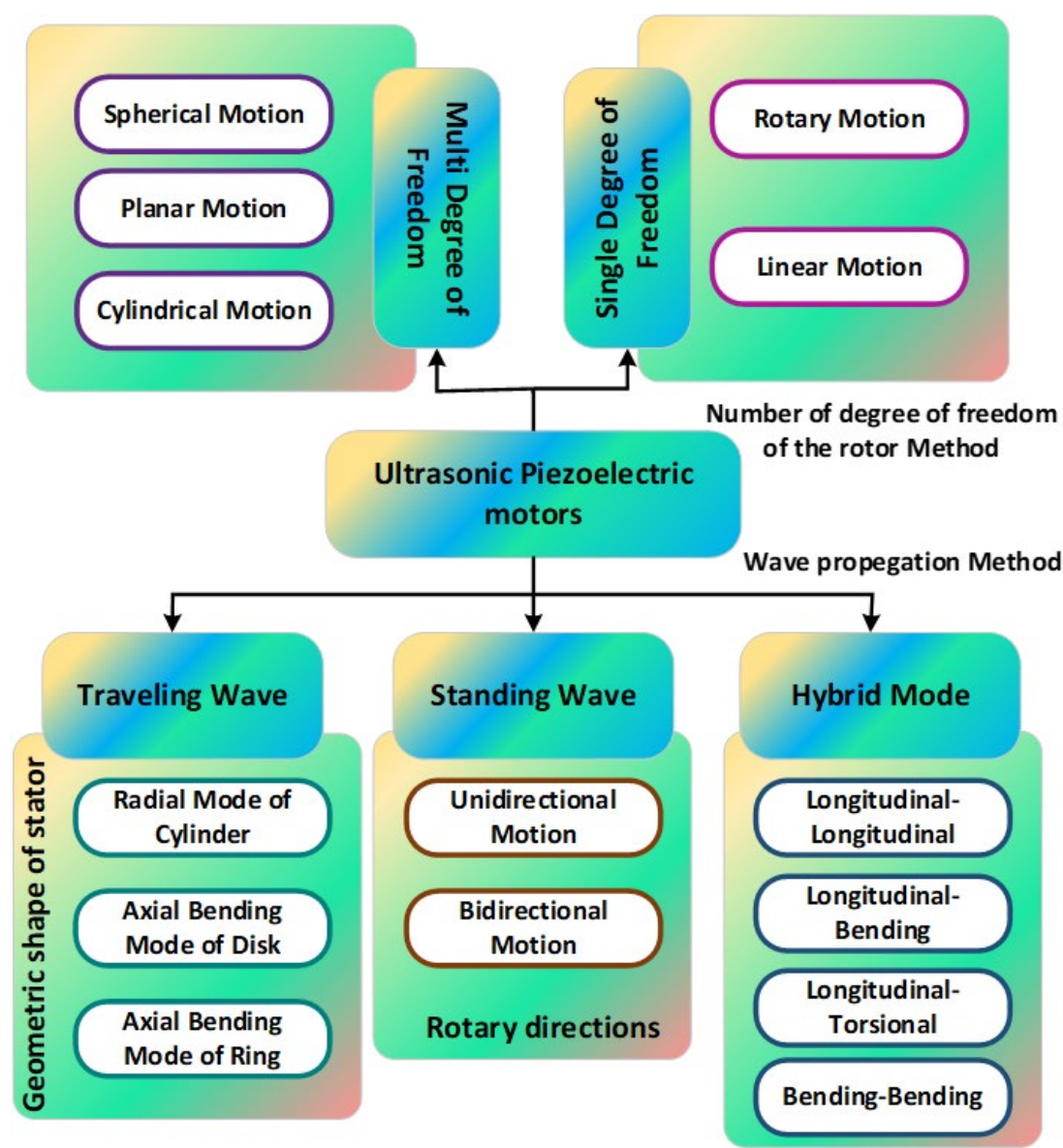


Figure 4. Classifications of USMs

Traveling wave motor.

When a traveling wave propagates through the stator, it causes elliptical motions on its surface. Figure 5 depicts the basic working concept of a traveling wave USMs where the driving foot is the point at which the stator and the runner make contact. The vertical amplitude of the traveling wave and driving foot are coincides. The driving foot's horizontal amplitude is related to the slope angle generated thru the moving wave and its distance among the stator's neutral layer and driving foot. A horizontal and vertical elements of driving foot are connected precisely as a traveling wave's slope angle and amplitude are. The stator's driving foot alternately drives the runner/rotor with its elliptic movements as the traveling wave spreads onward. Hence the runner moves against the other direction as the traveling wave moves. By overlapping of two standing waves a traveling wave is formed. The vibration superposition principle states that two standing waves should have identical vibrational structure, frequency, and amplitude, having a wavelength of one quarter variance in space and a distinction in phase of $\pm \pi/2$ over a period. The equations of vibration for traveling and standing waves are presented in equations. (5) to (7).

$$X_1 = k \sin\left(\frac{2\pi}{\zeta} y\right) \cos(\omega t) \quad (5)$$

$$X_2 = k \sin\left(\frac{2\pi}{\zeta} \left(y + \frac{\zeta}{4}\right)\right) \cos\left(\omega t + \frac{\pi}{2}\right) \quad (6)$$

$$X_3 = X_1 + X_2 = k \sin\left(\frac{2\pi}{\zeta} y - \omega t\right) \quad (7)$$

The mathematical representation of the standing waves is shown in equations (5) and (6), while the traveling wave is described in equation (7); symbol t denotes time; ζ is wavelength, ω indicates the angular frequency, and k symbolize standing wave's amplitude. It demonstrates that the traveling wave motor requires two sinusoidal stimulating impulses of the identical frequency with a phase alteration of $+\pi/2$ or $-\pi/2$. Furthermore, the two sinusoidal waves will stimulate the identical stator vibrational mode alongside an identical amplitude however, separated by a distance $\zeta/4$ in space. Changing the difference in phase between the excited signals causes the traveling wave to flow in the other way, reversing the direction of runner's moving. Therefore, the traveling wave motor can achieve bidirectional motion. The driving foot can regulate the magnitude of the elliptical movement thru varying the exciting signals voltages at the same time. It is worth noting that changing the voltage levels of both exciting signals would result in additional standing waves formed in the stator, that will have an influence on the circular driving foot's motion. The structure of elliptical movement remains constant since the amplitudes of vibrations of pressing and pushing both components are connected; this restricts the adaptability of modifying the traveling wave motor's output torque and speed.

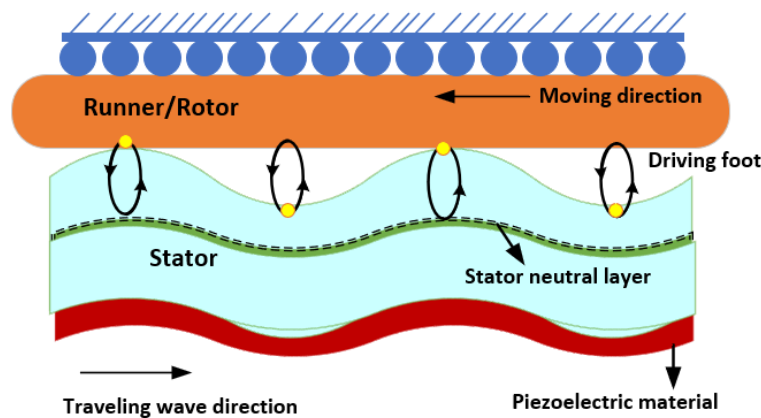


Figure 5. Operating principle of TUSMs.

Some performance analysis of the various state-of-the-art TUSMs are numerically illustrated in Table 3 where motion and type of stator, size of piezoelectric element, driving voltage, rotational velocity and speed, frequency, preload force and generated torque are shown for various proposed motors.

Table 3. Performances analysis of various TUSMs.

Reference	Year	Motion	Stator type	Size(piezoceramic)	Voltage	Velocity/Speed	Frequency	Force	Torque
[72]	2024	Rotary	Ring	12*5*2mm	500Vpp	62rpm	40kHz	10N	0.94Nm
[73]	2023	Linear	Disk	9*1.65*2.7mm	500Vpp	19.04rpm	19kHz	300N	1.2Nm
[74]	2023	-	Ring	0.5mm	200Vp	120rpm	41kHz	250N	1.1Nm
[75]	2023	-	Radial	3 μ m	6Vpp	>12000rpm	95.2kHz	50mN	14.89 μ Nm
[76]	2023	Rotary	Disk	<10 μ m	80Vp	158rpm	41.9kHz	40N	73Nmm
[77]	2023	Rotary	Disk	-	500V	153rpm	36.2kHz	280N	1.5Nm
[78]	2023	Linear	Cylinder	15*15mm	60Vpp	7.9mm/s	96kHz	-	-
[79]	2021	-	Ring	27*2*0.5mm	200Vp	128.2rpm	41kHz	250N	0.9Nm
[80]	2020	Rotary	-	7.5*4.2*1.5mm	250Vpp	53.86rpm	24.86kHz	0.69N	0.11Nm
[81]	2020	-	-	-	1.3Vpp	160rpm	41.5kHz	-	1Nm
[82]	2020	Rotary	Ring	340*180 μ m	-	17.09rpm	39.6kHz	250N	0.35Nm
[83]	2020		Ring	60mm	24Vp	110rpm	37.2kHz	200N	1.2Nm
[49]	2020	Linear	Disk	-	6Vpp	1.7mm/s	19.3kHz	-	-
[84]	2019	Rotary	Disk	60mm	30Vpp	90rpm	0-100kHz	60N	1.5Nm

* Vpp is the peak-peak voltage, Vp is the peak voltage.

2.2. Standing wave USMs

The driving foot's elliptical motion is created by generating a standing wave (also known as a mode shape) in the stator of ultrasonic piezoelectric motor[85]. The basic working mechanism of the standing wave ultrasonic motor is graphically demonstrated in figure 6. Despite the driving foot's pushing and pressing components are produced by the same exciting sinusoidal signal, the elliptical movement can be obtained due to the stator's damping ratios along the distinct directions of these component. As a small difference between the damping ratios, the motion trajectory typically degenerates into an almost straight line-like flat ellipse[86,87]. The oscillating driving foot's direction is consistently diagonal to the forward motion of the runner(rotor), ensuring that both components are sufficiently powerful to propel the runner. The runner's movement direction is governed thru the driving foot's vibrational direction. In figure 6, one may be clearly observed that driving foot's position and the stator's mode shape determine the direction of vibration for the standing wave motor. Both stator design and exciting frequency dictate the mode shapes. The driving foot goes diagonally when seen from the bottom left to the top right if it is positioned on the antinode's right side. Conversely, the driving foot will experience vibrations that travel from the right side of bottom to the left top, causing the runner to drive towards the left. In contrast to the generation of traveling waves in the stator of the TUSMs, the stator of the SUSMs may readily produce standing waves despite its geometry. The SUSMs may utilize rotors as runners for linear motion and sliders for

rotational motion. Therefore, several linear SUSMs [88,89,90] and rotary SUSMs[91,92,93] were proposed in state of the art, each exhibiting different vibration patterns in the stators. The SUSMs can further categorized into two types based on their output motions: unidirectional and bidirectional SUSMs. Some performance analysis of the various state-of-the-art SUSMs are numerically demonstrated in table 4 where vibrator, shape of stator, driving voltage, rotational velocity and speed, frequency, force are shown for various proposed motors. Figure 7 show the V-shaped standing wave ultrasonic piezoelectric motor represented by Xiandi et al [94] , where figure 7(a) shows the physical prototype photo of standing wave transducer, figure 7(b) shows the excitations appeared in motor, figure6(c) illustrates the excitation signals followed by the vibration direction, figure 7(d) represents the driving tip’s elliptical trajectory evolution along the phase difference, figure 7(e) demonstrates the ultrasonic testing setup, and figure 7(f) represents the complete experimental setup for standing wave ultrasonic motor.

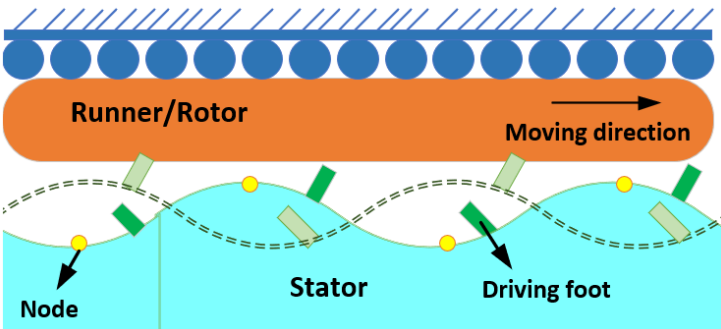


Figure 6. Basic operating principle of SUSMs.

Table 4. Performances analysis of various SUSMs.

Reference	Year	Vibrator	Stator shape	Voltage	Velocity/Speed	Frequency	Force
[95]	2023	-	V-shaped	90V	0.2m/s	32.2kHz	10N
[94]	2023	linear	V-shaped	80Vrms	0.23m/s	33kHz	20N
[96]	2023	linear	V-shaped	150V	-	39.1kHz	-
[97]	2021	linear	V-shaped	400Vrms	0.53m/s	39kHz	30N
[98]	2020	linear	V-shaped	350Vrms	1.27m/s	38.6kHz	80N

* Vrms is the root mean square voltage.

2.3. Hybrid modes USMs

Hybrid modes USMs (HUSMs) are USMs that use two distinct modes of operation to mimic elliptical motion of the driving foot, working mechanism of HUSMs is graphically demonstrated in figure 8. Where the driving foot oscillates in distinct ways in modes A and B. Based on the concepts of vibration superposition and Lissajous curves, the driving foot’s elliptical motion can be accomplished through stimulating modes A and B with two sin impulses at the identical frequency and with a specified phase variation (ϕ). To reverse the direction of rotation of the elliptical trajectory, flip the phase difference of the excited signals to $-\phi$. Hence, varying the phase difference allows the HUSMs to achieve bidirectional movements. Furthermore, the two exciting signals can separately change the pressing and pushing components of elliptical movement, which are subject by modes A and B, correspondingly. Therefore, the electrical voltage levels of the exciting signals may be used to modulate the HUSMs output speed and thrust with great versatility.

Table 5 numerically illustrates the performance of various state of the art presented HUSMs, contains the vibration or motion patterns, stator type, presented prototype dimensions, applied

voltage, obtained velocity and speed, operating frequency, and force. A hybrid mode ultrasonic piezoelectric motor is shown in figure 9 presented by Ziang et al[99], where figure 9(a) demonstrates the hybrid motor over all configuration, figure 9(b) illustrates that when longitudinal PZT plates are powered by phased voltages, the longitudinal traveling waves (LTW) travels in a pair of arms oriented over the x-axis, causing another arms pair (the passive arms) to produce bending vibration. Figure 9(c) describes the mesh structure relating to the LTWs, figure 9(d) shows the elliptical motions by bending standing waves (BSWs) in the xz and yz planes, and figure 9(e) illustrates the mesh shapes occurred by BSWs in vertical directions.

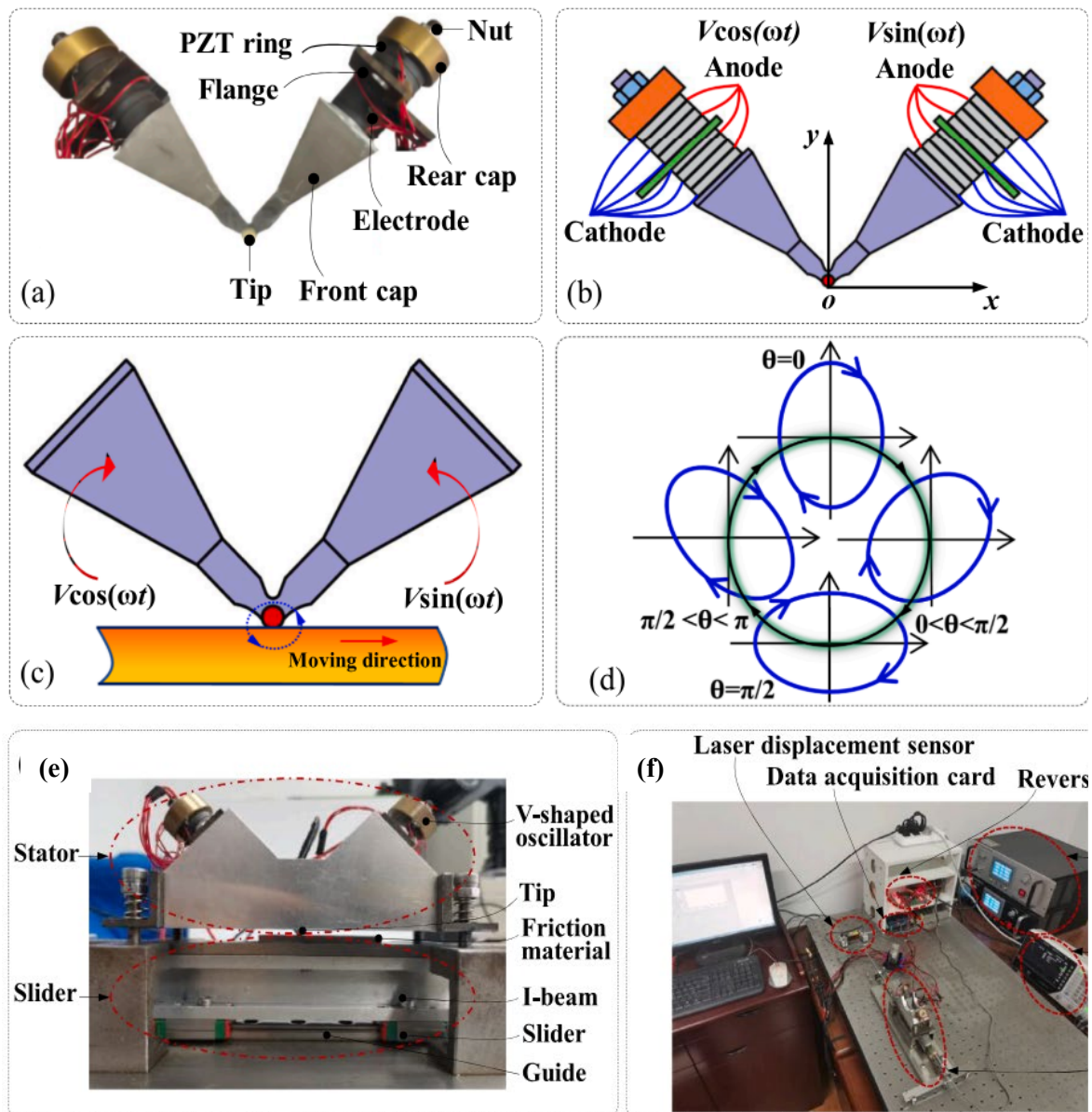


Figure 7. V-shaped vibrator of standing-wave linear ultrasonic motor: (a) proposed physical prototype motor, (b) motor in excitation mode, (c) the vibration following direction, (d) driving tip's elliptical trajectory progress along the phase difference, (e) testing ultrasonic motor prototype, and (f) complete experimental testing setup. [94].

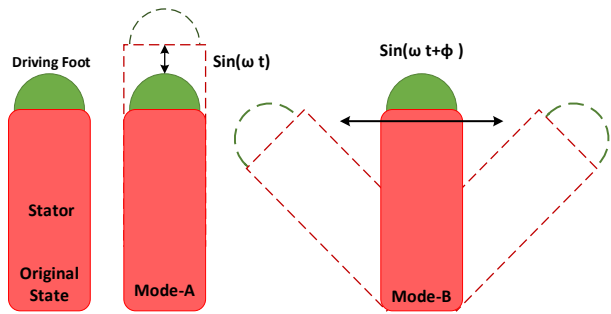


Figure 8. Basic working principle of HUSMs.

Table 5. Performances analysis of various HUSMs.

Reference	Year	Motion/Vibration	Stator structure	Prototype Size	Voltage	Velocity/Speed	Frequency	Force
[100]	2022	Longitudinal	tuning fork	-	320Vpp	88.67mm/s	80.2kHz	99mN
[101]	2022	Bending	-	45.7*30mm	180Vp	1103mm/s	30.2kHz	392mN
[102]	2020	Longitudinal	-	-	-	-	-	-
[102]	2020	Transverse-Shear	disk	2*10*4mm	300Vpp	169.4mm/s	24.7kHz	7.5N
[103]	2020	Longitudinal-torsional	cylinder	10*10*55mm	400Vpp	483rpm	56kHz	22N
[104]	2019	Bending-Bending	planar	20*44*30mm	400Vpp	300μm/s	40Hz	1.47N
[99]	2023	Longitudinal	disk	68*68*28mm ³	250V	877mm/s	27.4kHz	40.2N
[105]	2019	Bending	-	-	-	-	-	-
[105]	2019	Longitudinal-Bending	disk	40*112*38mm	400Vpp	124.2mm/s	1.4kHz	105N

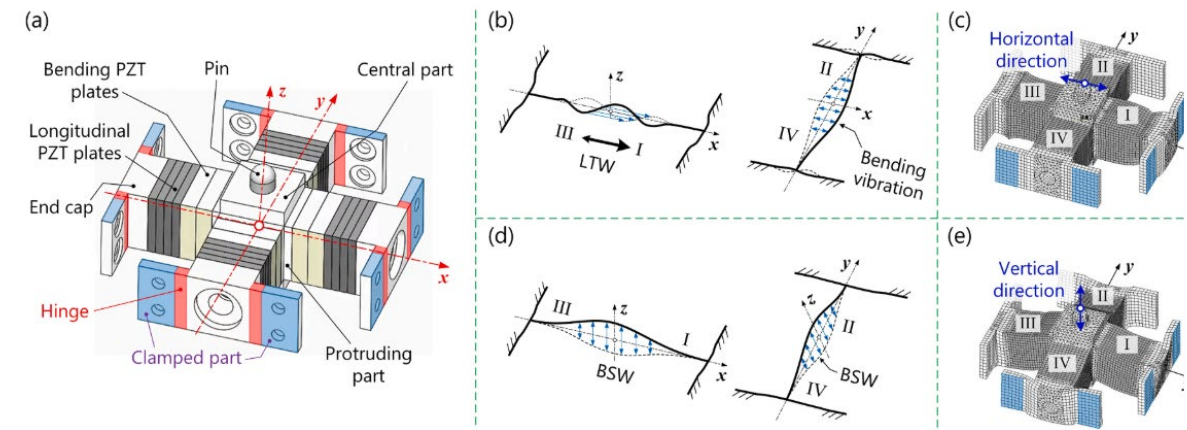


Figure 9. Hybrid mode ultrasonic piezoelectric motor: (a) the hybrid motor over all configuration, (b) when longitudinal PZT plates are powered by phased voltages, the longitudinal traveling waves (LTW) travels in a pair of arms oriented over the x-axis, causing another arms pair (the passive arms) to produce bending vibration, (c) the mesh structures related to the LTWs, (d) the elliptical motions by bending standing waves (BSWs), and (e) the mesh shapes occurred by BSWs in vertical directions.[99].

2.4. Multi-DOF piezoelectric ultrasonic motor

The further functions associated with the concurrent management of numerous degrees of freedom (DOF) inside a single mechanism of USMs provided the investigators with a particularly

extensive area of exploration[106,107]. Various multi-DOF-USMs are being described [108,109]who follow the core fundamentals of operation of the SUSMs, TUSMs, and HUSMs for the purpose of offering qualities such as nanometric resolution, self-braking, high controllability, rapid response time, and other similar characteristics. Several stators can work together to provide multi-DOF-USMs movements for the runner. The next sub-sections discuss three distinct categories of multi-DOF-USMs, including: Spherical, rotary-linear, and planar USMs, where rotary-linear and planar USMs have just two DOF while spherical USMs have two or three DOF.

2.4.1. Spherical USMs

S. Toyama invented one of the first 'spherical' USMs in 1991 [110], which was later enhanced [111]. The drive was designed for machine assembly, laser cutting, and use as an individual joint in robots. Recent advancements in MEMS technology and active piezoelectric materials have led to the development of expert spherical USMs. A bonded type longitudinal-bending mode spherical shape 2-DOF HUSM is presented to meet the needs for accurate movement along with control in a limited space for underwater and space applications [112]. The motor comprises a pyramid-shaped piezoelectric active elements mover and a friction base with a curved spherical shape that serves as the stator, where the prior loading force is generated by a tension spring underneath the piezoelectric mover. Functioning modes include the mover's bending and longitudinal vibrations. The geometry parameters were optimized using FEA of the motor. Where the experimental findings showed that the highest velocity of rotation in both x and y directions approached to 414 deg/s when the voltage used for excitation is 550 Vpp. Moreover, results also showed that the highest peak forces for the proposed spherical based 2-DOF HUSM in x and y directions are 5.25 N and 5.34 N, correspondingly, where the excitation voltage is 525 Vpp. Mizuno et al [107] presented spherical shaped stator base multi-DOF USMs utilizing rotational mode vibrational motion of the stator shown in figure 10(a), where 24 multilayer piezoelectric actuators are embedded on the surface of stator. Other highlighted spherical shape multi-DOF USMs are presented in [113,114,115].

2.4.2. Rotary-linear USMs

Linear and rotary are the two distinguished classes of USMs however, some multi-DOF USMs may produce both linear and angular motion [116,117]. A linear-rotary moment based USM is presented [118] for optical beam luminous flux density control. The motor features a single stator made of a piezoelectric bimorph disc and a carbon fiber cylindrical tube, attached in the center. The disk is perpendicular to its flat surface. Quadrilateral waveguides are generated in the inner circumference of a disc, aligning with the tangential direction of the cylindrical tube outer surface. This waveguide arrangement converts the radial vibrations of the bimorph disc into rotational oscillations of the cylindrical tube. The USM has two vibration modes: second out-of-plane bending and first radial. The carbon-based tube has a ring-shaped rotor that may be moved or rotated using the inertial principle. Another highlighted USM named precise linear-rotary positioning stage (LRPS) is presented by Chang et al [119] for optical focusing graphically shown in figure 10(b). This motor achieved both linear and rotational motions along and around the vertical directions respectively. Furthermore, an experimental study was conducted on the prototype of LRPS to evaluate its performance illustrated in figure 10(c). The experiment demonstrated that it could perform linear motion with a stroke of 5 mm and rotational motion with a stroke of 360°. The resolutions for upward and downward linear movements were 82.32 and 86.26 nm, respectively. The resolutions for clockwise and anticlockwise rotating rotations were 3.90 and 3.85 μ rad, respectively.

2.4.3. Planar USMs

The paper [120] describes a planer motion-based USM called twin coil spring-based soft actuator, which is powered by two flexible USMs. Each USM consists of a small metallic stator and an elastic, extended coil spring. It can travel forward and backward with extensibility and bend left and right with flexibility. The motor's basic operating concept is based on two vibrational modes: the

first mode repeats contraction and expansion symmetrically around the central cross-section, while the second mode is asymmetrical. The model has been experimentally examined, and it has demonstrated strong response characteristics, high sensor linearity, and resilience while maintaining flexibility and controllability in planer motion. Wentao et al[121] presented a bonded-type planer multi-DOF USMs which operates in both torsional and bending hybrid modes containing PZT plates. Its working principle is shown in figure 10(d), where the vibrations displacement occurred in all four directions. Another prominent study on planer type USM based on two-mode X-Y direction motion is represented [122].

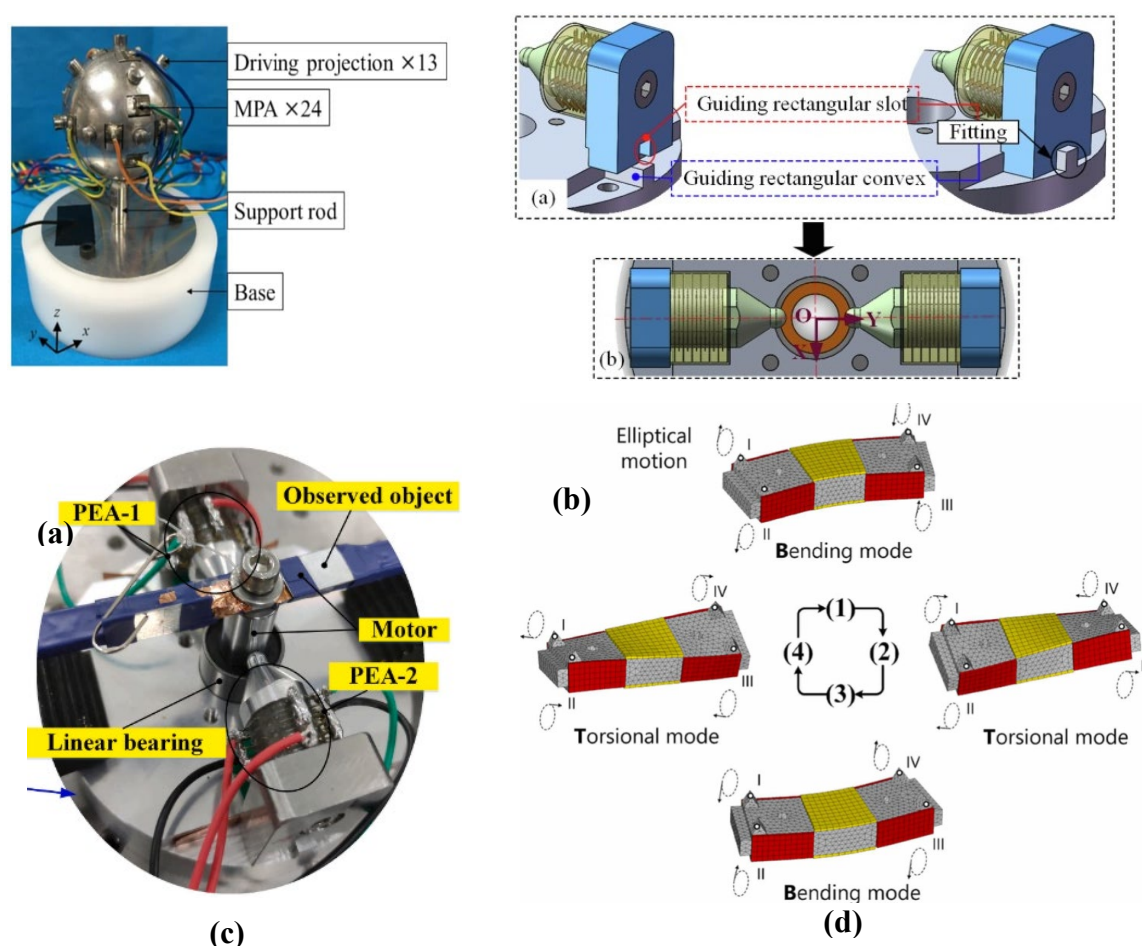


Figure 10. Multiple degree of freedom USMs: (a) Spherical stator bases multi-DOFUSMs [107], (b) Optical focus precise linear-rotary positioning stage (LRPS) prototype containing two piezoelectric actuators [119], (c) Experimental setup for LRPS [119], (d) Planer ultrasonic motor bending in four directions [121].

Finite Element Modeling of USMs

A finite element modeling (FEM) is important computational method for analyzing and forecasting USMs behavior. Before building actual prototypes, engineers can use it to realistically replicate the motor's efficiency under various operating situations. This method conserves resources as well as time during the design and implementation phase.

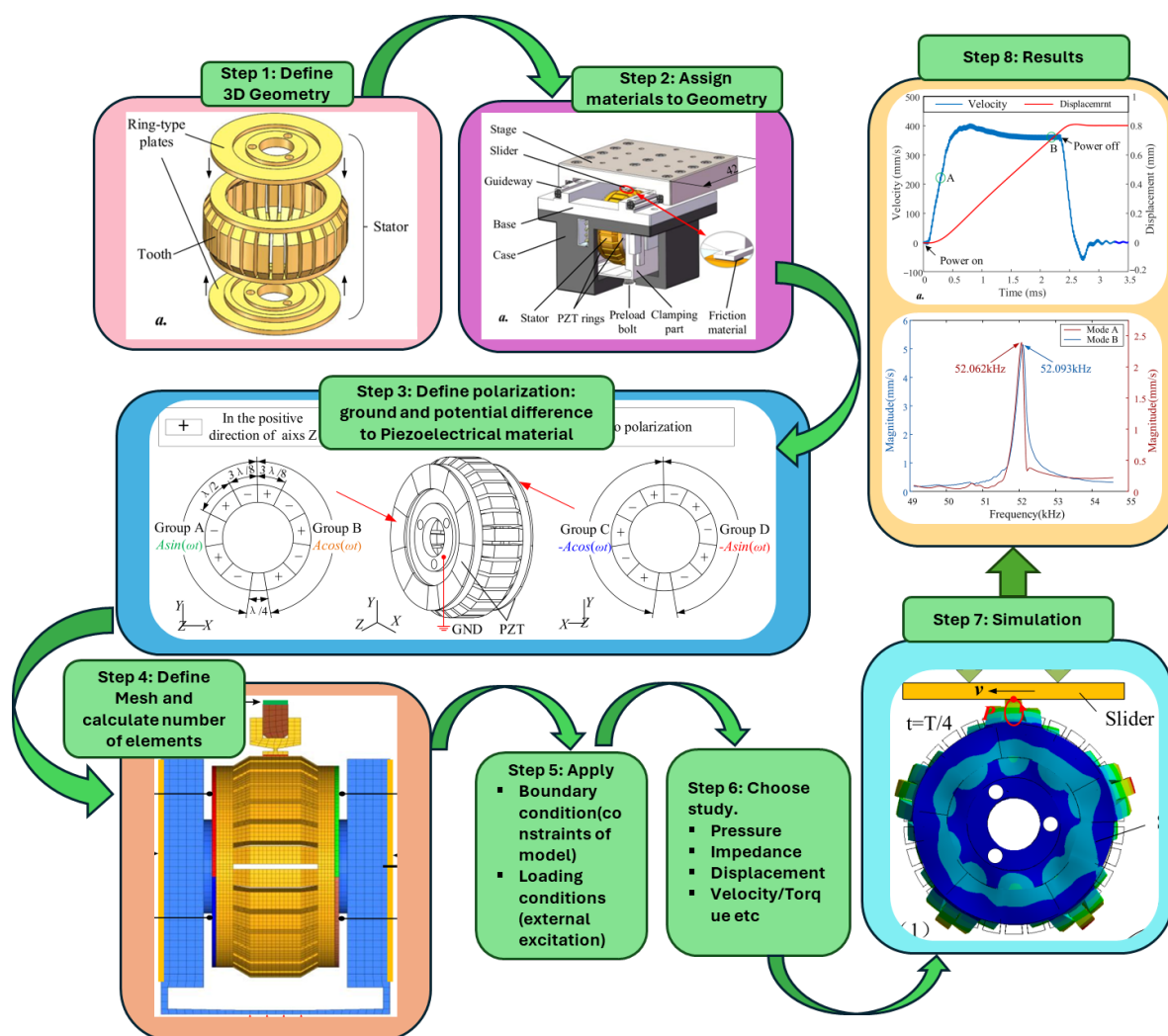


Figure 11. Steps of 3D Finite element modeling of USMs in multiphysics software.

The initial step of FEM is system modeling that includes to define geometry dimensions, material properties, mesh generation, boundary conditions and loading conditions. Once the system modeling is completed then analysis and results are carried out through simulations, which may include strain and stress distribution, model analysis and performance prediction. Torque/speed study under loading and unloading conditions, displacements, efficiency, and noise generations are the characteristics observed in performance prediction step. Various commercial software like COMSOL multiphysics, Ansys, ADINA, and Abaqus offers FEM features and tools to analysis the piezoelectric devices effectively. However, FEM for USMs still have some challenges, like careful consideration of material characteristics, boundary conditions, and non-linearities such as friction in the contact region are necessary to create an accurate FEM model. Furthermore, to execute simulations, sophisticated models with precise meshing may need a large amount of processing power and time. To make sure the model correctly depicts behavior in the actual world, experimental testing is required to validate the FEM results.

The first FEM of USMs was performed by Yamabuchi and Kagawa[123] in 1989 in order to analyze the piezoelectric elastic structures and represent the study to understand qualitatively characteristics of the ultrasonic motor. Later in 1992, Maeno et al. shed light on the mechanical properties of the ring type ultrasonic motor by FEM code MSCINASTRAN to determine the real ring-type stator's vibration mode [124]. In 1996, another study was presented to looked at how the piezoceramic's shape affects the stator's vibration by FEM [125]. Where a detailed geometry was considered to compute the electrical excitation and mechanical vibration in the stator of USM. In last two decades a lot of work has been done on FEM of USMs to get more advance, efficient and

optimized designs. The highlighted work includes model analysis to demonstrate the elliptical vibration process [14,103,126,127]. The major steps of FEM of USMs are graphically demonstrated in Figure 11 and design and modeling figure were taken from the FEM study presented by Yang et al.[128].

Fabrication methods of USMs

Several considerations, such as the intended USMs size, functionality, and cost, influence the fabrication technique selection. Larger USMs are usually utilize bulk machined methods while thin-film manufacturing method works better for micro scale USMs.

Conventional fabrication methods of USMs

The conventional technique known as "bulk machining" consists of the milling process of the ceramic or metal parts that make up the stator and rotor. With adhesives, the piezoelectric components are then attached to the stator. This process consists of two main steps: machining and piezoelectric element attachment. The machining process consists of grinding, milling, or turning techniques to manufacture stator and rotor from the desire material like stainless steel, aluminum, ceramic etc. It guarantees that every component has exact measurements and desire shape. The vibration-producing piezoelectric ceramic components are then firmly attached to the stator with the use of adhesives such as epoxy. Adhesives must be carefully chosen and applied in order to enable adequate vibration transmission and prevent the introduction of stress spots that might cause cracking.

Jing et al. used hollow design fabricated method to get a hollow structure stator instead of using bolts and glues to connect different parts of stators [129].

Major benefits of this approach are good for mass manufacturing and provides excellent accuracy. It enables precise rotor and stator shape and tight tolerances which are required for effective motor functioning. The comparatively straightforward and well-established methodologies of this technology make it ideal for high-volume manufacture of USMs. While its main drawbacks are that it can be laborious, time complicated and challenging bonding, particularly for micromachined USMs. The bonding procedure must be well thought out. A poor choice or application of glue can result in weak joints, obstruct vibration transmission, or introduce stress concentrations that could lead to fractures in the motor parts.

Micro and nano fabrication methods of USMs

Techniques for fabricating micro and nanoscale materials provide benefits for intricate designs and downsizing. A major essential techniques are thin-film deposition, micromachining, and lithographie galvanofomung abformung(LGA). Several considerations influence the choice of micro or nano manufacturing technique, notably the necessary performance of the motor, the size and complexity of the desired feature, the material's suitability to the piezoelectric film, and the volume and cost of production [130,131]. The techniques, advantages and considerations of these nano/micro fabrication methods are listed in table 6.

A thin-film deposition method utilizing processes like chemical vapor deposition (CVD), sputtering, and electrohydrodynamic jet printing (EHJ printing), in order to directly deposit a thin film of piezoelectric materials onto a printing surface. Atoms that form a thin layer on the substrate are ejected using sputtering processes, which use a high-energy laser to target the piezoelectric material. Precursor chemicals are introduced using CVD, and they react and break down on the substrate to generate the appropriate piezoelectric layer. Piezoelectric ink with suspended particles is applied onto the substrate by EHJ Printing using an electric field. Micromachining entails the use of several methods, including Reactive ion etching (RIE), photolithography, and deep reactive ion etching (DRIE), for removing material from a substrate to produce the required USMs geometries. Figure 12 shows the basic steps of micro machining fabrication process for thin-film micro motor. Zhou et al. presented a MEMS (Microelectromechanical systems) technology based on silicon wafer

consist of metal decomposition, etching, and sputtering [132]. Another highlighted MEMS technology-based fabrication was presented by Yang et al. for thin film piezoelectric micromotor[133].

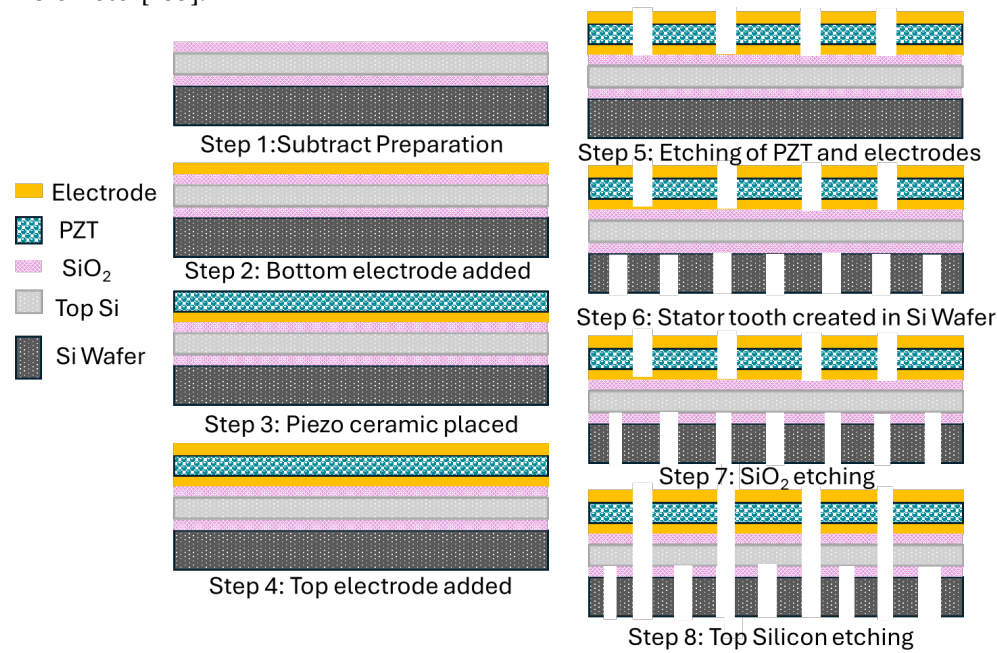


Figure 12. Basic steps of micro machining fabrication process for thin-film micro motor.

The first miniature tube ultrasonic motor was fabricated by Uchino[134,135,136], the motor was fabricated in three different designs by reducing its size, the total length of tube ultrasonic motor of 1st design was 10mm, 2nd design was 6mm and 3rd design was 4mm shown in Figure 13. Kohei et al utilized the micromachining technology to produce a small stator of dimensions of (0.41 mm × 0.41 mm × 0.25 mm). The success of the stator manufacturing process is attributed to a micromanipulator that can regulate a small quantity of glue in a sub-milligram order [137]. Another highlighted miniature ultrasonic motor was fabricated by Shunsuke et al for-focus systems[138].

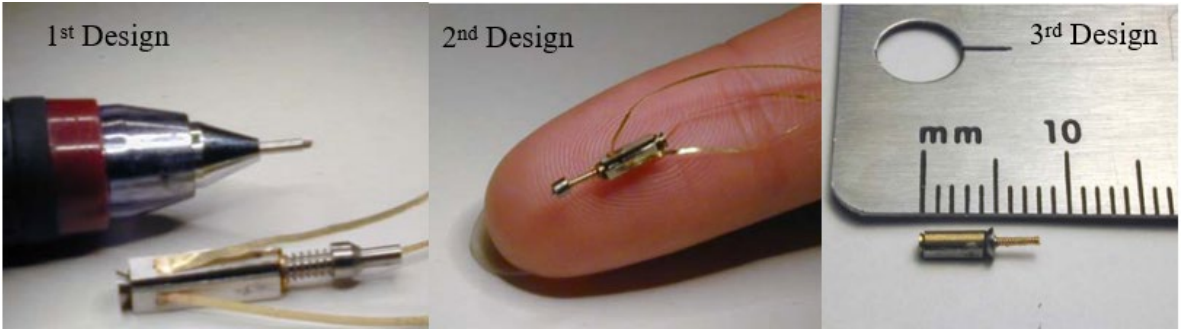


Figure 13. Miniature tube USMs presented by Uchino in various dimensions[135].

Table 6. List of various techniques for micro/nano fabrication methods along with their advantages and considerations.

Method	Techniques	Considerations	Advantages
Thin-Film Deposition	<ul style="list-style-type: none">➤ CVD,➤ Sputtering,EHJ Printing	Cost, Performance of thin films, Dedicated apparatus	Complex designs, Miniaturization, Remove the need of bonding process

LGA	<ul style="list-style-type: none"> ➤ X-ray lithography, ➤ Electroplating, molding 	Expert tools, Complex process, limited materials	Good quality surface, Raised proportions of aspects of metal structures
Micromachining	<ul style="list-style-type: none"> ➤ RIE, ➤ Photolithography, ➤ DRIE 	Surface roughness, Multi-step process, residual stress	Intricate characteristics, Combines thin-film deposition processes

"Lithographie Galvanoformung Abformung," (LGA) is the German acronym that translates to "X-ray lithography, electroplating, and molding." A high-resolution resist design is made on a substrate using X-ray radiation in this procedure. A thick coating of metal is electroplated onto the patterned resist. Following that, the resist is removed, revealing a metallic mold with a high aspect ratio. The USMs stator with exact characteristics may then be created by casting molten metal into the mold.

Characterizations of USMs

USMs may be characterized using a variety of techniques to assess their functionality and performance. Such as performance, dynamic and material characterization. These characterization techniques offer insightful information about the capabilities, effectiveness, and constraints of USMs. The kind of USM being analyzed and the sought information determine which specific approaches should be used. List various characterization methods of USMs is shown figure 14. Below is a summary of several important methods.

Performance Characterization

The study of torque, speed, and efficiency measurement of USMs are carried out in performance characterization. Torque measurement, which gauges the motor's rotary force at various speeds and loading scenarios, is an essential component of motor characterization. These techniques include the use of torque meters or custom test configurations. The ability to detect the motor shaft's speed of rotation utilizing a variety of tools, such as encoders[135], tachometers, or laser doppler vibrometers (LDV)[130] for high-precision applications, is another crucial feature. To calculate the motor's energy conversion efficiency, the electrical power input and mechanical power output must be measured. In contrast, high-accuracy linear displacement (travel distance) is determined in displacement measurement utilizing laser interferometry or linear encoders. The performance characterization of various proposed USMs are shown in tables 3,4 and 5.

Material Characterization

This characterization involves piezoelectric coefficient and tribological measurements of USMs. The ability of the stator's piezoelectric material to transform electrical power into vibratory motion is measured using the piezoelectric coefficient. To evaluate this attribute, specialized tools are employed. Tribological characterization measures the wear and friction characteristics of the materials of the rotor and stator. Tribometers and wear pattern analysis in simulated operating circumstances are used in these procedures. Kohei et al performed a characterization of microscale ultrasonic motor with rotor dimension of 0.15mm diameter and obtained 5.4nNm maximum torque and 714 rad/s angular velocity by applying a voltage of 44.8V_{pp}. This characterization was performed with hard/soft PZT and lead magnesium niobate-lead zirconate titanate (PMN-PT)_ piezoelectric materials for the transient response study shown in figure 15 [137].

Dynamic Characterization

In dynamic characterization usually frequency response and resonance analysis based techniques are applied to study important characteristics of USMs. The assessment of frequency

response determines the motor's reaction to varying driving frequencies. By employing frequency sweep techniques and examining output torque or fluctuations in speed, it may be quantified. Resonant frequencies of the motor are identified using resonance analysis, which is important since they might affect stability and performance. Vibration patterns or changes in electrical impedance are measured using these approaches. Shunsuke et al. performed the characterization of thin hollow linear ultrasonic motor for lens focus systems and studies transient response, force and velocity characteristics of motor shown in figure 16. [138]

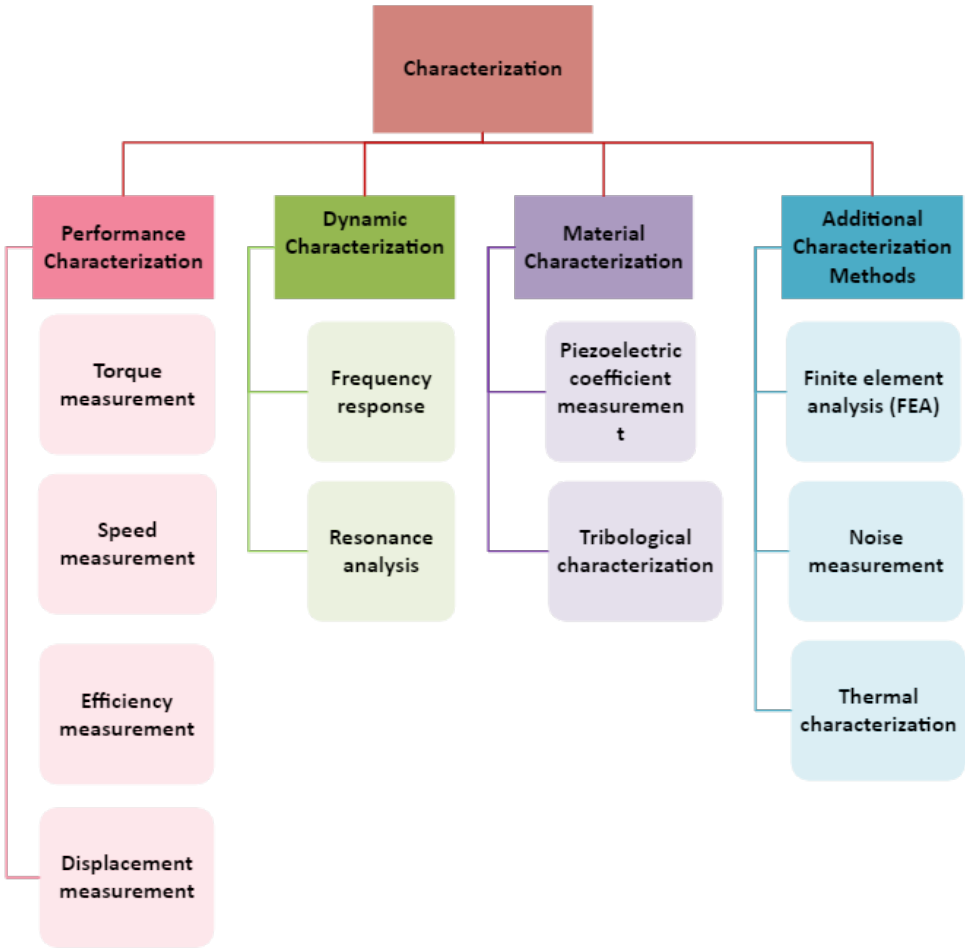


Figure 14. Various characterization methos of USMs.

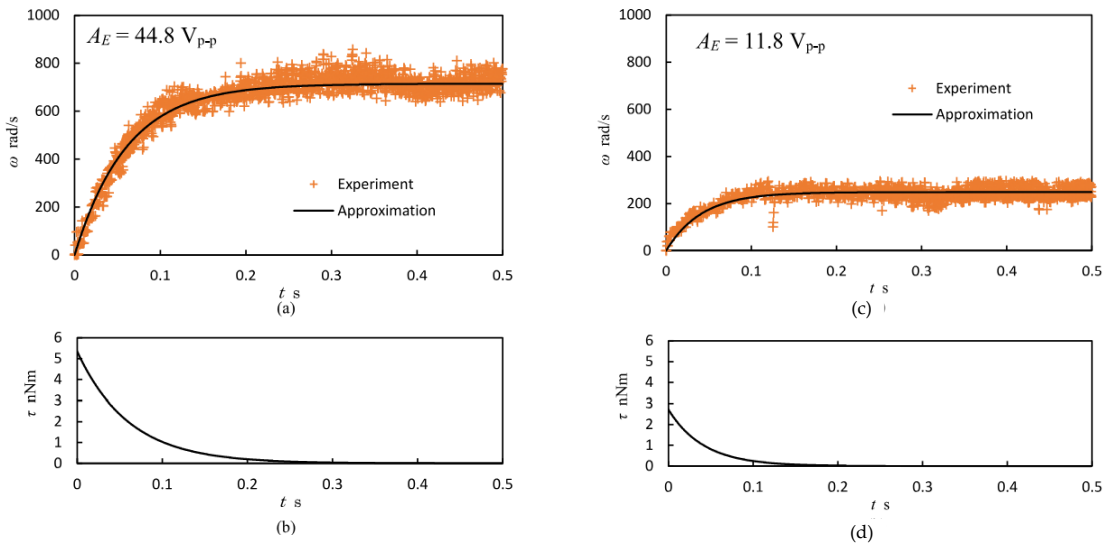


Figure 15. The micromotor's transient reaction (a) experiments and least minimal approach for hard PZT, (b) the torque derived from the angular velocity curve approximation for hard PZT, (c) experiments and the least minimal approach for PMN-PT, (d) the torque derived from the angular velocity curve approximation for PMN-PT.[137].

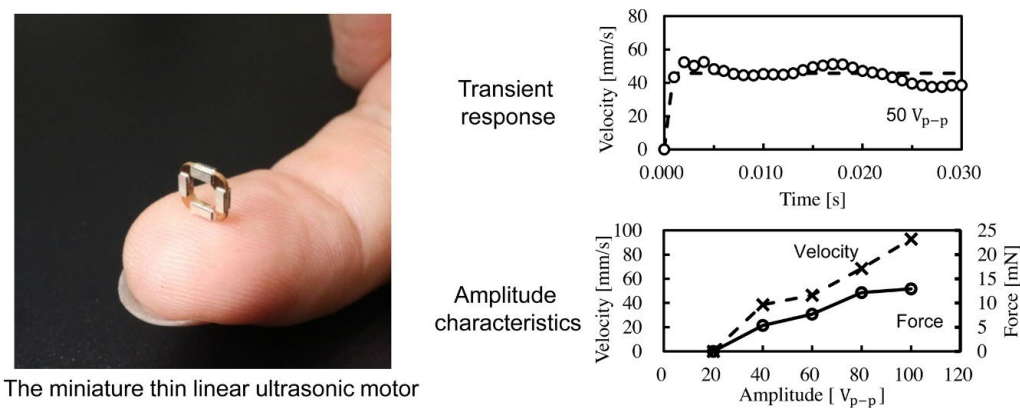


Figure 16. Characterization of hollow ultrasonic miniature motor for lens used in focus systems.[138].

Table 7. Equipment and techniques used for various characterization of USMs.

Characteristic	Equipment	Technique
Torque	Torque meter, Load Cell [130,134]	Static or Dynamic Load Application, [132] Pre-Load mechanisms Custom test configuration
Speed Velocity	Tachometer, Laser doppler vibrometer, [133] encoders	Transient characterization method [130,135] Direct Measurement, Frequency Sweep Techniques
Efficiency	Power Supply, Load Cell, Tachometer, Multimeter	Calculation of Mechanical Output Power / Electrical Input Power, Frequency Sweep Techniques Torque*angular speed/ Input power [136]
Vibration	Accelerometer, Laser Scanner Vibrometer	Measurement of Vibration Levels and Patterns [131]
Strain	Strain Gauge, Digital Image Correlation, Interferometry	Non-contact optical method High-precision technique
Temperature	Thermocouple or Thermistor	Monitoring Temperature Distribution
Noise	Sound Level Meter	Measurement of Acoustic Noise
Electric parameters	Multimeter	Direct measurement of current and voltage
Friction and Wear	Tribometer	Simulation of Operating Conditions

Piezoelectric coefficient	Berlincourt Meter, d33 Meter, Laser Interferometry	Quasi-static method
Holding Force	Load Cell	Measurement of Maximum Static Load
Frequency Response	Signal Generator, Power Amplifier, laser Doppler vibrometer, Spectrum Analyzer	Inputting Varying Frequency Signals and Measuring Response
Resonance	Signal Generator, Power Amplifier, laser Doppler vibrometer, Spectrum Analyzer	Identification of Resonant Frequencies and Mode Shapes, Frequency Sweep Techniques
Impedance	Impedance analyzer[138], LCR meter, Network analyzer, Oscilloscope	Direct Measurement, Vectorial Measurements, S-Parameters[139]
Displacement Angular acceleration	linear variable differential transformer, Laser Triangulation sensor, laser displacement sensor, laser interferometer, linear encoder	Measurement of Linear or Angular Displacement[131] Newton second law[135]
Quality factor	Bode plot	Bode plot[131]

Applications of USMs

USMs occupy a particular gap in numerous fields by providing a combination of high precision and control, fast response and speed, quiet operation, EMI free operation, compact size, and clean operation [140,141]. These attributes render them indispensable for jobs necessitating precise control, rapidity, and efficient operation within a compact framework [142,143,144]. Thus, the ultrasonic motor has been used in fields such as semiconductor manufacturing [145,146], textile and printing machinery [147,148,149,150], ultrasonic cleaning and drying [151,152,153], aerospace [154,155,156], robotics [120,157,158], endoscopy[159], intelligent surgical robots [160,161], optical fiber [162,163], biomedical engineering [140], magnetic resonance images[164,165], artificial intelligence [166,167], laser surface texturing [94] etc. Figure 17 illustrates the various application of USMs. In this section, the detail utilization of USMs in the fields of surgical robots, industrial, aerospace, and biomedical is provided. Table 8 shows the importance of each characteristic of USMs in the fields of surgical robots, industrial, aerospace, and biomedical.

Surgical Robots based on USMs

USMs serve an important role in minimally invasive surgery. The noteworthy advantages of these surgeries include a decrease in post-operative discomfort, diminished risks during and after

surgery, shorter hospital stays, faster healing, fewer cuts and scars, less immune system stress, and shorter surgical times and total expenses [168,169]. A broad range of nano and microscale medical ultrasonic robots have been revealed in last decade to approach and transcend the level of biological tools used for general surgeries in the pancreas, liver, intestines, gallbladder ducts, cardiovascular, spinal, and genital areas. Furthermore, various research investigations are being undertaken in oncological surgeries, such as urology, and lung surgery. Moreover, some of these models dealt with detecting tumoral lesions and establishing resection margins, while others were meant to assess the viability of ultrasound-guided surgeries. A few studies also assessed the robotic drop-in probe, the consistency of the hepatic tissue, and the circulatory flow in the pulmonary vein [170]. A millimeter-scale rolling microrobot is designed for gastrin testimonial tracks and arteries. Driven by a micro ultrasonic motor and a micro planetary gear train, it can produce 60 μNm torque and 4500 rpm speed. The prototype measures 14 mm in length, 10 mm in width, and 7 mm in height, and weighs 640 mg. Experiments showed that the microrobot maintains speed on slopes with high friction coefficient, even on low friction slopes [171].

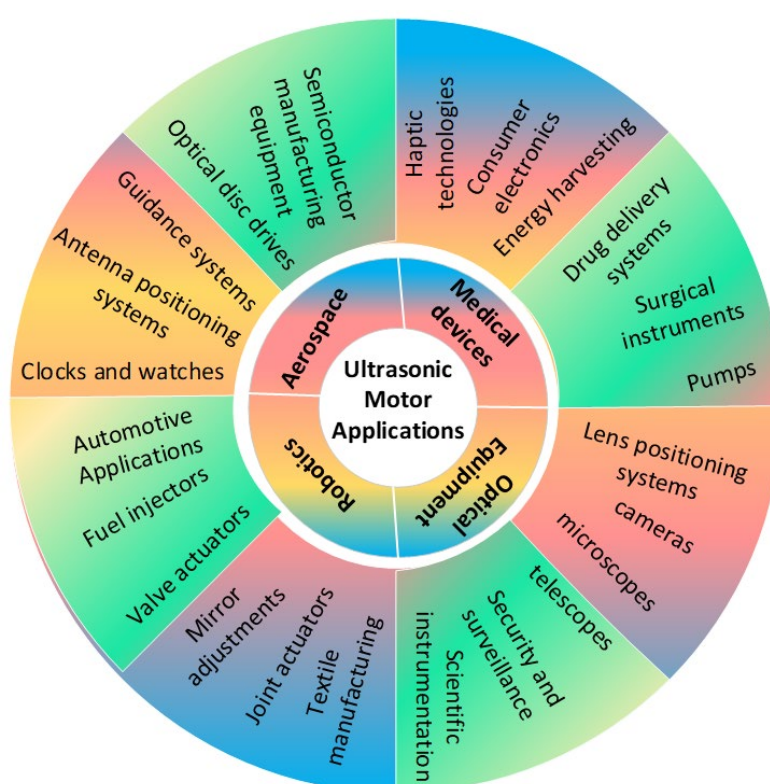


Figure 17. Various application of USMs.

Laparoscopic surgery

Electromechanical rotatory USMs based on piezoelectric material are commonly employed in laparoscopic single-site operations owing to their tiny wound size, wide field of vision (FoV), ease of repetitive high positioning precision, small dimension, and fast response [172,173]. The authors describe a novel three degree of freedom laparoscopic surgical robot (LSR) powered by a double-leg ultrasonic motor (DUM) containing piezoelectric ceramic active plates in order to induced longitudinal and bending coupling vibrations. The two-stage, three-order bending vibrations can form a traveling wave that drives the DUM rotor. A genetic algorithm-II is used to optimized the DUM stator, leading to increased moving stability and driving efficiency. The mechanical properties of DUM have been investigated experimentally. The maximum no-load rotational speeds are 333.75 and 335.77 rpm for clockwise and counterclockwise rotation respectively, with maximum output torques of 2 and 1.6 N mm. The experimental platform is designed to demonstrate that LSR may alter its posture to get a proper surgical FoV, demonstrating that the use of DUM in LSR has substantial

benefits and potential [174]. Katsuhiko et al. suggested a soft actuator with a cylindrical cam mechanism that converts linear to rotating movement for laparoscopic surgery. In laparoscopic surgery, a tiny rotating actuator was mounted on the edge of a forceps manipulator, resulting 3Nmm torque with a 70° angle of rotation. The actuator has the benefit of being easily sterilized and disposable [175].

Neurosurgery

For conducting robotic neurosurgery, the ultrasonic piezoelectric motor is noticeably favored part of the system, especially in microsurgery and stereotactic procedures. It shows several benefits, including nonferrous material, tiny size, strong holding torque, and quiet operation. A researcher develops magnetic resonance (MR) conditional parallel robot consists of a 3-degree-of-freedom translational and remote center of motion (RCM) modules by using the actuation capabilities of USMs [176]. A model evaluation based on genetic algorithm is performed in order to obtained maximize dexterity then prototype fabrication and experimental verification is carried out. The RCM module's orientation stability was measured to be $0.055\pm0.0016^\circ$, with an absolute orientation inaccuracy of $2.05\pm0.019^\circ$. The robot's impact on the signal-to-noise ratio in images obtained from MR imaging is less than 4%, demonstrating a high potential application in MR-restricted neurosurgery. Another flexible surgical robot that uses beacon total focusing technique (b-TFM) to enable high-accuracy ultrasonic position sensing and strong magnetic steering is presented [177]. This robot demonstrates the ability to drive nimbly. A 1 mm x 1 mm PZT patch inserted on the tip of the robot which determine the robot's location. The ultrasonic position sensing system used in the model oversee the entire navigation process, with a maximum error of 0.8 mm at a steering radius of 100 mm. Moreover, USMs have proven frequently employed in MRI-guided robotic systems to increase accuracy by legitimate the system's uncertainties and nonlinearities due to its MR safety properties [178,179]. For example, the positioning accuracy can be effectually reduced to sub-degree level thru particularly developed controllers [180,181].

Cardiovascular Surgery

A hollow ultrasonic motor (HUM) is successfully utilized in Master-slave vascular interventional robotic systems for minimally invasive cardio surgery. The goal of the vascular interventional robotic system using a hollow ultrasonic motor, is to provide physicians the ability to carry out intricate vascular procedures precisely and dependably. The proposed slave robot is made up of a linear movement platform and a hollow drive mechanism which relies on a traveling wave ultrasonic motor. The stator of HUM, optimized by an evolutionary algorithm for superior quality and larger amplitude of traveling waves, which are beneficial to the drive efficiency, eliminates the need for a redundant transmission mechanism and maintains beneficial co-axiality due to its property of a high positional precision, and fast response. The overall Master-slave vascular interventional robotic systems feature High kinematic accuracy, little hysteresis, and excellent cooperative performance [158].

Table 8. Importance of various characteristics of ultrasonic motor in various applications.

Characteristic	Importance	Fields	Applications
High Precision & Resolution	Allows precise and intricate motions,	Minimally invasive surgery	Instrument control
	allowing for accurate placement and	Aerospace	Antenna pointing, Telescope adjustment
	providing	Biomedical engineering	Drug delivery, Microfluidic devices
	manipulation at the micrometer scale.	Industrial automation	Robotic assembly,

			Laser cutting
Fast Response & Speed	Enables fast operating and swift adjustments in position through the use of speedy start-stop and motion functions.	Industrial automation	Assembly lines, Material handling
		Biomedical engineering	Pumps, Microfluidic devices
Silent Operation	Essential for locations that are sensitive to noise by producing minimum noise.	Minimally invasive surgery	Improved Patient Comfort, Quieter surgical environment, Improved Communication and Collaboration of surgical teams
		Biomedical engineering	Medical pumps, Diagnostic Equipment, Implantable Devices
		Aerospace	Minimizing acoustic disturbances, Microgravity Experiments,
No electromagnetic interference (EMI)	Ensures optimal performance in the proximity of delicate electronic devices while preventing electromagnetic interference (EMI) disturbances.	Biomedical engineering	Implantable devices
		Industrial automation	Environments with sensitive electronics, Medical Device Production and Assembly, Applications Requiring Sparks or Flammable Materials
			Safeguarding sensitive Electronics, Compatibility with scientific Equipment, Reduced Risk of Signal Interference
		Aerospace	
Compact Size & Lightweight	Enables the reduction in size of instruments and decreases the total weight.	Minimally invasive surgery	Surgical tools
		Aerospace	Spacecraft design
		Biomedical engineering	Implantable devices
Harsh Environment Tolerance	Capable of functioning in harsh conditions such as severe temperatures, radiation, and vacuum, making it	Aerospace	Satellite components, Deployment mechanisms

	indispensable for space operations.		
Low Power Consumption	Conserves energy and prolongs battery lifespan in circumstances with limited resources.	Aerospace	Spacecraft design
		Biomedical engineering	Implantable devices

Industrial Applications

USMs have gained a lot of popularity in industrial environment and are extensively employed in numerous industries, like chemical processes, machinery, automobile, aerospace because of their appealing characteristics, such as small structure, quick response, excellent accuracy, the intrinsic virtuous electromechanical coupling factor, compatibility in extreme environment, producing massive force and, their other mechanical aptitudes [182]. To meet the growing demand for USMs, that are capable of adapting to harsh environments, the purpose of [154] was to investigate the factors that lead to the deterioration of performance and the failure mechanism of an ultrasonic motor when it is exposed to a shock environment. A physical experiment and a finite element modeling simulation are carried out in order to investigate the effect on an ultrasonic motor. This investigation includes the environmental influence on the mechanical characteristic of an ultrasonic motor as well as the vibration characteristic of a stator. In addition, the protective effect of rubber on an ultrasonic motor in a distress environment is demonstrated by the use of an experimental approach. In [183] , a nonlinear dynamics model and identification approach are described for the purpose of designing a driver circuit for high voltage excitation applications in industrial settings. The outcomes of the experiments indicate that there is a reduction in harmonic distortion below 500 Vpp, which enables a higher motor output power. A highly small camera module that is employed as an image stabilizer and for security systems has been studied and developed over the course of many years, particularly with regard to their minimized size, related output force, speed, and maximum output power demand for a variety of loads. The experimental research that was conducted in [184]focused on simple bimorph and multi-layer bimorph USMs. According to the findings, the thrust was as high as 3.08 N and 2.57 N, with a satisfactory free speed and structural thicknesses of 0.7 and 0.6 mm, respectively. In addition, the design that has been suggested has a significant potential for the use of the smartphone camera module, particularly in the field of moving sensor image stabilization. A [185] presents a minuscule, ring-shaped linear USM with a single, in-plane E01 mode in order to generate the accurate precision suitable for changing temperature environments. The motor has a peak driving force of 2.7 N, output power of 18.6mW, a no-load driving velocity of ~56 mm/s, and a precise position/displacement accuracy of 0.1 μm under open-loop control. The presented linear motor's simple shape, broad bidirectional operating stroke, and adjustable micrometer-scale displacement proving that it has tremendous promise for manufacturing applications particularly precise actuations. A four-leg USMs model consisting of eight PZT sheets is described in [186], providing a high voltage two-phase signal excitation. The four ceramic feet efficiently moved a slider in a straight path. A 600 × 160 mm prototype was created for experimental purposes. The testing findings demonstrate that a 200 V driving voltage provide a maximal translated speed of 135 mm/s and an effective force of 3.6 N making it an intriguing choice for precise and industrial applications due to its size, features and great output efficiency.

Aerospace Applications

USMs possess a distinctive blend of accuracy, dependability, and effectiveness, rendering them extremely advantageous for a wide range of aerospace applications. Due to their impeccable performance in the harsh environments of space and their tiny dimensions and energy-efficient

design, they are highly favored for space exploration missions. In aerospace these USMs are used for satellite systems, deployable mechanisms, telescopes and other optical instruments, micro positioning tasks, samples manipulation, and exploration or maintenance robotic systems. Xinchu et al describes a unique rotary ultrasonic motor based on numerous Langevin transducers that is intended for long-term, steady operation in aeronautical systems. The study of motor's maximal no-load speed with pre-pressure is carried out, and observed that it has excellent loading performance, rapid reaction capacity, high displacement angle resolution while retaining miniature. Setting the driving voltage 350Vpp, with variation of pre-pressure 10 N and 60 N, yields a no-load speed of 62 and 34 rpm respectively. It shows that as the pre-pressure rises to 60 N, the no-load maximal speed drops. The motor's start/stop response period is 4.6/5.5 milliseconds [187]. Another design strategy of rotary traveling wave ultrasonic motor was developed based on the bending mode of a ring-shaped stator that used less PZT ceramics to minimize bulk and increase mechanical output properties. The two standing waves and driving tips' motion patterns were calculated. The motor achieved an output speed of 53.86 rpm with a preload of 0.69 N at 24.86 kHz and 250 Vpp. The highest stall torque was 0.11 Nm at 3.14 N. Furthermore, this study was compared to a prior design, and it was discovered that the volume was greatly decreased, additionally, system efficiency, the no-load speed, torque, and power density were increased considerably [188]. Another research was carried out to examine the driving properties of the built-in sandwich traveling wave transducer that was proposed. To construct a traveling wave piezoelectric motor, the rotor was driven by the transducer that was presented. Also performed were tests on the motor prototype's output performance. The experimental findings showed that with a pre-pressure of 300 N, a voltage of 500 Vpp, and an exciting frequency of 19 kHz, the motor's no-load speed was 19.04 rpm, its stall torque was 1.2 Nm, the machine's maximum output power was 0.6453 W, and the highest possible output efficiency was 15.87%. The dependable operation of the drive application and the practicality of the transducer structure design method were further confirmed by the normal functioning of the rotating motor [189]. USM is also being investigated as wireless motors based on traveling waves due to their flexibility, excellent durability, and convenience for aerospace applications. A stated solution seamlessly integrates capacitive power transmission into a USM to provide a newly created not magnetic wireless direct-drive motor. In contrast with previous wireless motors, the suggested wireless USM prevents the use of delicate microcontrollers and passive or active controls on the motor side, allowing for complete control on the primary side, enabling high-degree integration and zero-maintenance process. Furthermore, bidirectional motion capabilities and adjustable speed regulation may be easily obtained by varying the amplitude and sequence of two-phase outputs on the primary side, allowing for a true sensation of wireless direct drive. Moreover, conceptual evaluation and practical testing are shown to demonstrate the practicality of the proposed wireless USM for aircraft applications [190]. The authors propose a viable technique to build friction-stress management and energy conversion augmentation toward an energy-saving and high-efficiency friction USMs used in aerospace technology. The model describes a low-voltage rotating USM which utilizes laser-induced microtextured stators and flexible rotors and achieved 158 rpm and 73 Nmm torque at 80Vp with 40 N preload [191]. To meet the high reliability requirements of aerospace applications, a unique traveling wave rotary USM with a ceramic support capability (Backup motor) is developed. Two USM models a cantilever-tooth backup motor (CTBM) and a modified backup motor with straight-tooth (STBM) were developed and built, utilizing electromechanical characteristics of PZT. These models performed in standard, backup, and boosted modes depending on the excitation parameters of the PZTs. Finite element analysis and prototype testing were used to investigate the links between the performance of three different working modes. The outcomes reveal that backup mode, as a substitute, closely matches the performance of regular mode, however boosted mode clearly outperforms the others. Extreme working trials further validate the effect of decreasing stress on PZT degradation. The comparison of two distinct types of motors shows that STBMs can deliver greater frictional drive achievement [192]. A low-voltage driving traveling wave USM containing multilayer four piezoelectric ceramics is proposed to excite 2-twisting modes at the same frequency corresponding to the motor. Experimental studies were conducted to examine the

stator's vibration features, and the mechanical output characteristics of the proposed model. Analysis showed that the motor can operate at voltages that are as little as 5 volts (pp). A long stroke was executed, exhibiting maximum forward and backward rotational velocities of 187.7 and 176.6 rpm respectively. Additionally, a peak stalling torque of 4.8 Nm was attained at 47.3 kHz while operating at 15 V_{pp} [193]. Moreover, a detachable stator constructed using the fine-blanking technique is provided. Experimental findings reveal that the maximum rotating speed is 150 rpm, and the highest stalling torque is 1.42 Nm, demonstrating the stator structure's fine-operating performance and rationale. The study reveals that the detachable stator made by fine-blanking technology has a promising future in the ultrasonic motor application sector [194].

Biomedical Applications

The recent advancements in biomedical sciences, with the shrinking of microelectromechanical devices, there is a growing need for multipurpose control of chip portions and biological cells. Traditional multiaxial phases are inadequate for multipurpose manipulation, requiring numerous manipulators. These precision mobile robots are not suitable to miniaturize multifunction operation because of their complex connecting wires. Therefore, USMs are practical controllers for creating wireless robots since their energy efficiency is significantly greater than that of other millimeter-scale motors. An omnidirectional mobile robot named Δ -type driven by USM is proposed and investigated its capabilities experimentally, by positioning deviation, velocity, and getting consistency of translational motions under open-loop conditions. The Δ -type robot accomplishes velocities ranging from 18.6-31.4 mm/s and repeatability of 4.1%-9.1% having a weight of 200 g. Where the repeatability is calculated as the ratio of the finishing points' standard deviation to the mean route length [157].

Piezoelectric USMs Trends and Future developments

The future of piezoelectric USMs seems promising, as there is a growing need for smaller, more accurate, and efficient motors in several industries. Below are few prospective future trends in piezoelectric USMs.

Material advancements

- **New piezoelectric materials:** Researchers are now working on creating new piezoelectric materials that possess enhanced characteristics such as increased efficiency, a broader range of operating temperatures, and improved resistance to fatigue. This will result in USMs that have improved performance and a broader range of uses.
- **Composite materials:** Ongoing research is being conducted on composite materials that integrate the piezoelectric effect with additional advantageous characteristics such as lightweight construction or stiffness. These composite materials have the potential to enable the development of USMs with distinct and specialized capabilities.

Miniaturization and integration

- **Micro-USMs:** Miniaturizing USMs, especially for use in micro-robots, healthcare equipment, and hydrodynamic systems, is a significant current development. The invention of micromachining and fabrication processes will facilitate the production of increasingly miniature and accurate USMs.
- **Integration with other technologies:** USMs are being combined with other microelectromechanical systems (MEMS) devices and sensors to form more intricate and versatile systems. These advancements will create opportunities for the development of new applications in fields like as biotechnology and aviation.

Improved control and performance

- **Advanced control algorithms:** The growth of advanced control algorithms will enable the more accurate and efficient functioning of USMs. This will enhance their productivity and empower them to tackle more intricate tasks.

- **Higher torque and speed:** USMs are continuously enhanced to attain greater torque and speed characteristics. This will increase their potential for use in areas such as manufacturing automation and robotics.
- **Self-sensing USMs:** Ongoing research is being conducted on USMs that possess the ability to perceive their own internal state and adapt their functioning accordingly. This would improve the quality and durability in a wide range of applications.

New application areas

- **Medical devices:** Miniaturized USMs show potential for application in surgical instruments, pharmaceutical delivery devices, and precise manipulation duties inside the human body.
- **Nanotechnology:** USMs have the potential to manipulate and position items at the nanoscale, which could lead to significant improvements in nanorobotics and material science.
- **Energy harvesting:** USMs serve as energy harvesters, transforming surrounding vibrations into electrical energy. This technology has the potential to be used in powering low-energy devices such as wearable electronics and wireless sensor networks.
- **Smart cities:** USMs have the potential to have a substantial impact on the development of smart cities. Their capabilities extend beyond basic automation, making a significant contribution to the development of a sustainable, customized, and adaptable urban environment. Envision a system of self-repairing infrastructure, where embedded USMs in buildings or roads initiate repairs upon sensing damage, or a network of microfluidic channels driven by USMs that gather real-time environmental data. USMs have the potential to allow building facades to adapt to weather conditions and to generate customized experiences in public spaces using equipment that can be rearranged. USMs could potentially improve waste management by providing the power needed for robotic sorting systems or autonomous collection bots. To create a more peaceful urban environment, USMs could be included into active noise cancellation systems in designated areas or even public transit vehicles. USMs could be advantageous in traffic management by implementing them in dynamic traffic light actuators to enhance traffic flow optimization. The potential is extensive, and as USM technology progresses in conjunction with the idea of optimal smart cities, we may anticipate the development of even more innovative and influential applications.

Challenges and considerations

- **Manufacturing complexity:** Advanced manufacturing processes are necessary for the shrinking and integration of USMs, but they can be costly and difficult.
- **Material limitations:** The characteristics of existing piezoelectric materials impose restrictions on the capabilities of USMs in certain domains. Ongoing investigation into novel materials is essential.
- **Cost reduction:** Reducing the manufacturing expenses of USMs will be essential for their extensive implementation in many different industries.
- **Cryogenic applications:** Extreme temperature transducers are necessary to operate in cryogenic conditions that are colder as -230°C and higher up to 125°C , specifically for aerospace technologies. PMN-PT will be the good option due to its operational flexible rang of cure temperature additionally its multilayer structure will enhance the torque power density of USMs[195,196].
Ultimately, the future prospect for piezoelectric USMs is favorable. Due to progress in materials, downsizing, control techniques, and the emergence of new applications, USMs are on the verge of becoming even more adaptable and essential tools in many different sectors.

Conclusions

An USM is a form of actuator that converts vibration into rotational or translational motions by employing high-frequency ultrasonic waves. These USMs provide a unique characteristic like high precision and speed, quiet operation, non-magnetic, simple design, and versatility that make them valuable for lot of applications. Piezoelectric material is the main driver of USMs due to utilizing its property of converting electrical energy into mechanical vibration. This review paper describes the importance of piezoelectric material for USMs, advantages of these USMs over other traditional motors like coil or magnetic field based, and characteristics of these motors. It describes several types

of USMs which includes traveling wave, standing wave, hybrid mode ultrasonic waves, multi-degree of freedom motors, and provides their basic operating mechanisms, utilization, and performance analysis of existing USMs. The design modeling like 3D finite element modeling and fabrications of USMs including conventional, micro/nano fabrication methods, and their characterizations are discussed briefly. USMs have a lot of applications in industrial and engineering fields due to their small size, enhanced precision and high controllability. Furthermore, a review on several highlighted applications including industrial, aerospace, robotics, and biomedical applications of USMs are addressed. Lastly future trends and challenges considerations including material advancement, size miniaturization, integration with other devices, improvement in control and performance are elaborated.

Author Contributions: Sidra Naz; conceptualization; data curation; writing—original draft preparation; investigation, Tian-Bing Xu; review and editing; resources; supervision; project administration; funding acquisition,

Funding: “This research was sponsored by the Office of Naval Research and was accomplished under Grant Number W911NF-23-1-0177”.

Data Availability Statement: No new data were created.

Conflicts of Interest: “The authors declare no conflicts of interest.”

References

1. L. Capineri and A. Bulletti, “Ultrasonic Guided-Waves Sensors and Integrated Structural Health Monitoring Systems for Impact Detection and Localization: A Review,” *Sensors*, vol. 21, no. 9, p. 2929, Apr. 2021, doi: 10.3390/s21092929.
2. M. Mazalan, A. Noor, Y. Wahab, S. Yahud, and W. Zaman, “Current Development in Interdigital Transducer (IDT) Surface Acoustic Wave Devices for Live Cell In Vitro Studies: A Review,” *Micromachines (Basel)*, vol. 13, no. 1, p. 30, Dec. 2021, doi: 10.3390/mi13010030.
3. H. X. Cao, V. Du Nguyen, J.-O. Park, E. Choi, and B. Kang, “Acoustic Actuators for the Manipulation of Micro/Nanorobots: State-of-the-Art and Future Outlooks,” *Micromachines (Basel)*, vol. 15, no. 2, p. 186, Jan. 2024, doi: 10.3390/mi15020186.
4. D. Mandal and S. Banerjee, “Surface Acoustic Wave (SAW) Sensors: Physics, Materials, and Applications,” *Sensors*, vol. 22, no. 3, p. 820, Jan. 2022, doi: 10.3390/s22030820.
5. Z. Guan *et al.*, “A self-powered acoustic sensor excited by ultrasonic wave for detecting and locating underwater ultrasonic sources,” *Nano Energy*, vol. 104, p. 107879, Dec. 2022, doi: 10.1016/j.nanoen.2022.107879.
6. A. Čeponis, V. Jūrėnas, and D. Mažeika, “Low Profile Triangle-Shaped Piezoelectric Rotary Motor,” *Micromachines (Basel)*, vol. 15, no. 1, p. 132, Jan. 2024, doi: 10.3390/mi15010132.
7. Y.-H. Wang, S. C.-S. Tsai, and F. C.-F. Lin, “Reduction of Blood Loss by Means of the Cavitron Ultrasonic Surgical Aspirator for Thoracoscopic Salvage Anatomic Lung Resections,” *Cancers (Basel)*, vol. 15, no. 16, p. 4069, Aug. 2023, doi: 10.3390/cancers15164069.
8. J. Zhang, Y. Wang, T. Liu, K. Yang, and H. Jin, “A Flexible Ultrasound Scanning System for Minimally Invasive Spinal Surgery Navigation,” *IEEE Trans Med Robot Bionics*, vol. 3, no. 2, pp. 426–435, May 2021, doi: 10.1109/TMRB.2021.3075750.
9. D. Zhang *et al.*, “Diagnostic Value of Multi-Mode Ultrasonic Flow Imaging Examination in Solid Renal Tumors of Different Sizes,” *J Clin Med*, vol. 12, no. 2, p. 566, Jan. 2023, doi: 10.3390/jcm12020566.
10. J. Qian *et al.*, “Ultrasound-Assisted Enzymatic Protein Hydrolysis in Food Processing: Mechanism and Parameters,” *Foods*, vol. 12, no. 21, p. 4027, Nov. 2023, doi: 10.3390/foods12214027.
11. Y. Li *et al.*, “An Ultrasound–Fenton Process for the Degradation of 2,4,6-Trinitrotoluene,” *Int J Environ Res Public Health*, vol. 20, no. 4, p. 3102, Feb. 2023, doi: 10.3390/ijerph20043102.
12. M. Salimi *et al.*, “Experimental and Numerical Investigation of the Use of Ultrasonic Waves to Assist Laser Welding,” *Materials*, vol. 17, no. 11, p. 2521, May 2024, doi: 10.3390/ma17112521.
13. J. Qiu, Y. Yang, X. Hong, P. Vasiljev, D. Mazeika, and S. Borodinas, “A Disc-Type High Speed Rotary Ultrasonic Motor with Internal Contact Teeth,” *Applied Sciences*, vol. 11, no. 5, p. 2386, Mar. 2021, doi: 10.3390/app11052386.
14. D. Xu, W. Yang, X. Zhang, and S. Yu, “Design and Performance Evaluation of a Single-Phase Driven Ultrasonic Motor Using Bending-Bending Vibrations,” *Micromachines (Basel)*, vol. 12, no. 8, p. 853, Jul. 2021, doi: 10.3390/mi12080853.

15. A. Zameer, S. Naz, and M. A. Z. Raja, "Parallel differential evolution paradigm for multilayer electromechanical device optimization," *Modern Physics Letters B*, Mar. 2024, doi: 10.1142/S0217984924503123.
16. S. Naz, A. Zameer, M. A. Z. Raja, and K. Muhammad, "Weighted differential evolution heuristics for improved multilayer piezoelectric transducer design," *Appl Soft Comput*, vol. 113, p. 107835, Dec. 2021, doi: 10.1016/j.asoc.2021.107835.
17. A. Zameer, S. Naz, M. A. Z. Raja, J. Hafeez, and N. Ali, "Neuro-Evolutionary Framework for Design Optimization of Two-Phase Transducer with Genetic Algorithms," *Micromachines (Basel)*, vol. 14, no. 9, p. 1677, Aug. 2023, doi: 10.3390/mi14091677.
18. S. Naz, A. Usman, A. Zameer, K. Muhammad, and M. A. Z. Raja, "Efficient multivariate optimization of an ultrasonic transducer with genetic parallel algorithms," *Waves in Random and Complex Media*, pp. 1–25, Sep. 2023, doi: 10.1080/17455030.2023.2256889.
19. S. Naz, M. A. Z. Raja, A. Mehmood, A. Zameer, and M. Shoaib, "Neuro-intelligent networks for Bouc–Wen hysteresis model for piezostage actuator," *The European Physical Journal Plus*, vol. 136, no. 4, p. 396, Apr. 2021, doi: 10.1140/epjp/s13360-021-01382-3.
20. S. Naz, M. A. Z. Raja, A. Mehmood, and A. Z. Jaafery, "Intelligent Predictive Solution Dynamics for Dahl Hysteresis Model of Piezoelectric Actuator," *Micromachines (Basel)*, vol. 13, no. 12, p. 2205, Dec. 2022, doi: 10.3390/mi13122205.
21. Z. Zheng *et al.*, "Micro-Electro-Mechanical Systems Microphones: A Brief Review Emphasizing Recent Advances in Audible Spectrum Applications," *Micromachines (Basel)*, vol. 15, no. 3, p. 352, Feb. 2024, doi: 10.3390/mi15030352.
22. A. C. Hatfield and T.-B. Xu, "Transparent Piezoelectric LiNbO₃-based Surface Acoustic Wave for Dust Mitigation in Space Environment," in *AIAA SCITECH 2023 Forum*, Reston, Virginia: American Institute of Aeronautics and Astronautics, Jan. 2023. doi: 10.2514/6.2023-0059.
23. G. Ali and F. Mohd-Yasin, "Comprehensive Noise Modeling of Piezoelectric Charge Accelerometer with Signal Conditioning Circuit," *Micromachines (Basel)*, vol. 15, no. 2, p. 283, Feb. 2024, doi: 10.3390/mi15020283.
24. Q.-T. Lai, Q.-J. Sun, Z. Tang, X.-G. Tang, and X.-H. Zhao, "Conjugated Polymer-Based Nanocomposites for Pressure Sensors," *Molecules*, vol. 28, no. 4, p. 1627, Feb. 2023, doi: 10.3390/molecules28041627.
25. S. Bouhedma, J. Bin Taufik, F. Lange, M. Ouali, H. Seitz, and D. Hohlfeld, "Different Scenarios of Autonomous Operation of an Environmental Sensor Node Using a Piezoelectric-Vibration-Based Energy Harvester," *Sensors*, vol. 24, no. 4, p. 1338, Feb. 2024, doi: 10.3390/s24041338.
26. C. Chen, T.-B. Xu, A. Yazdani, and J.-Q. Sun, "A high density piezoelectric energy harvesting device from highway traffic — System design and road test," *Appl Energy*, vol. 299, p. 117331, Oct. 2021, doi: 10.1016/j.apenergy.2021.117331.
27. Q. Qiao, X. Wang, W. Liu, and H. Yang, "Defect Detection in Grouting Sleeve Grouting Material by Piezoelectric Wave Method," *Buildings*, vol. 14, no. 3, p. 629, Feb. 2024, doi: 10.3390/buildings14030629.
28. I. Izadgoshasb, "Piezoelectric Energy Harvesting towards Self-Powered Internet of Things (IoT) Sensors in Smart Cities," *Sensors*, vol. 21, no. 24, p. 8332, Dec. 2021, doi: 10.3390/s21248332.
29. Z. Abdullah, S. Naz, M. A. Z. Raja, and A. Zameer, "Design of wideband tonpizl transducers for underwater SONAR applications with finite element model," *Applied Acoustics*, vol. 183, p. 108293, Dec. 2021, doi: 10.1016/j.apacoust.2021.108293.
30. L. Shams and T.-B. Xu, "Underwater communication acoustic transducers: a technology review," in *Sensors and Smart Structures Technologies for Civil, Mechanical, and Aerospace Systems 2023*, Z. Su, M. P. Limongelli, and B. Glisic, Eds., SPIE, Apr. 2023, p. 8. doi: 10.1117/12.2663073.
31. S. Naz, M. A. Z. Raja, A. Kausar, A. Zameer, A. Mehmood, and M. Shoaib, "Dynamics of nonlinear cantilever piezoelectric–mechanical system: An intelligent computational approach," *Math Comput Simul*, vol. 196, pp. 88–113, Jun. 2022, doi: 10.1016/j.matcom.2022.01.011.
32. A. Kausar, C.-Y. Chang, M. A. Z. Raja, A. Zameer, and M. Shoaib, "Novel design of recurrent neural network for the dynamical of nonlinear piezoelectric cantilever mass–beam model," *The European Physical Journal Plus*, vol. 139, no. 1, p. 16, Jan. 2024, doi: 10.1140/epjp/s13360-023-04708-5.
33. F. Qian, T.-B. Xu, and L. Zuo, "Piezoelectric energy harvesting from human walking using a two-stage amplification mechanism," *Energy*, vol. 189, p. 116140, Dec. 2019, doi: 10.1016/j.energy.2019.116140.
34. J. Lin, P. Yuan, R. Lin, X. Xue, M. Chen, and L. Xing, "A Self-Powered Lactate Sensor Based on the Piezoelectric Effect for Assessing Tumor Development," *Sensors*, vol. 24, no. 7, p. 2161, Mar. 2024, doi: 10.3390/s24072161.
35. J. Wang *et al.*, "Design and Analysis of a Cardioid Flow Tube Valveless Piezoelectric Pump for Medical Applications," *Sensors*, vol. 24, no. 1, p. 122, Dec. 2023, doi: 10.3390/s24010122.
36. J. Wallaschek, "Piezoelectric Ultrasonic Motors," *J Intell Mater Syst Struct*, vol. 6, no. 1, pp. 71–83, Jan. 1995, doi: 10.1177/1045389X9500600110.
37. M. Hunstig, "Piezoelectric Inertia Motors—A Critical Review of History, Concepts, Design, Applications, and Perspectives," *Actuators*, vol. 6, no. 1, p. 7, Feb. 2017, doi: 10.3390/act6010007.

38. chunsheng zhao, *Ultrasonic motors: technologies and applications*. Springer Science & Business Media., 2011. Accessed: May 17, 2024. [Online]. Available: https://books.google.com/books?hl=en&lr=&id=gVbGGkT5emgC&oi=fnd&pg=PR4&dq=ultrasonic+motor+s+technologies+and+applications+by+chunsheng+zhao&ots=4R_kqVr56E&sig=mPLMjASJ2kyu5IWkW4iA2c6vVqQ#v=onepage&q=ultrasonic%20motors%20technologies%20and%20applications%20by%20chunsheng%20zhao&f=false
39. A. Shuaibu Ahmad, M. Mukhtar Usman, S. Bello Abubakar, and A. Yusuf Gidado, "Review on the application of Piezoelectric materials in the development of ultrasonic motors," *Journal of Advanced Research in Applied Mechanics Journal homepage*, vol. 33, no. 1, pp. 9–19, 2017, [Online]. Available: www.akademiabaru.com/aram.html
40. K. Spanner and B. Koc, "Piezoelectric Motors, an Overview," *Actuators*, vol. 5, no. 1, p. 6, Feb. 2016, doi: 10.3390/act5010006.
41. D. Xu, Y. Liu, S. Shi, J. Liu, W. Chen, and L. Wang, "Development of a Nonresonant Piezoelectric Motor With Nanometer Resolution Driving Ability," *IEEE/ASME Transactions on Mechatronics*, vol. 23, no. 1, pp. 444–451, Feb. 2018, doi: 10.1109/TMECH.2018.2790923.
42. M. V. Golub, S. I. Fomenko, P. E. Usov, and A. A. Eremin, "Elastic Waves Excitation and Focusing by a Piezoelectric Transducer with Intermediate Layered Elastic Metamaterials with and without Periodic Arrays of Interfacial Voids," *Sensors*, vol. 23, no. 24, p. 9747, Dec. 2023, doi: 10.3390/s23249747.
43. Y. Wang, S. Wu, W. Wang, T. Wu, and X. Li, "Piezoelectric Micromachined Ultrasonic Transducers with Micro-Hole Inter-Etch and Sealing Process on (111) Silicon Wafer," *Micromachines (Basel)*, vol. 15, no. 4, p. 482, Mar. 2024, doi: 10.3390/mi15040482.
44. A. U. H. Mohsan *et al.*, "Design and Effect of Resonant Ultrasonic Vibration-Assisted Laser Cladding (R-UVALC) on AlCrFeMnNi High-Entropy Alloy," *Materials*, vol. 17, no. 5, p. 969, Feb. 2024, doi: 10.3390/ma17050969.
45. L. Gou *et al.*, "Investigation of New Accelerometer Based on Capacitive Micromachined Ultrasonic Transducer (CMUT) with Ring-Perforation Membrane," *Micromachines (Basel)*, vol. 15, no. 2, p. 279, Feb. 2024, doi: 10.3390/mi15020279.
46. A. Wellendorf, L. von Damnitz, A. W. Nuri, D. Anders, and S. Trampnau, "Determination of the Temperature-Dependent Resonance Behavior of Ultrasonic Transducers Using the Finite-Element Method," *Journal of Vibration Engineering & Technologies*, vol. 12, no. 2, pp. 1277–1290, Feb. 2024, doi: 10.1007/s42417-023-00906-8.
47. Y. Liu, M. Hafezi, and A. Feeney, "A cascaded Nitinol Langevin transducer for resonance stability at elevated temperatures," *Ultrasonics*, vol. 137, p. 107201, Feb. 2024, doi: 10.1016/j.ultras.2023.107201.
48. M. Taşlıyol, S. Öncü, and M. E. Turan, "An implementation of class D inverter for ultrasonic transducer mixed powder mixture," *Ultrason Sonochem*, vol. 104, p. 106838, Mar. 2024, doi: 10.1016/j.ultsonch.2024.106838.
49. V. Ruiz-Díez, J. Hernando-García, J. Toledo, A. Ababneh, H. Seidel, and J. L. Sánchez-Rojas, "Bidirectional Linear Motion by Travelling Waves on Legged Piezoelectric Microfabricated Plates," *Micromachines (Basel)*, vol. 11, no. 5, p. 517, May 2020, doi: 10.3390/mi11050517.
50. C. Peng, H. Wu, S. Kim, X. Dai, and X. Jiang, "Recent Advances in Transducers for Intravascular Ultrasound (IVUS) Imaging," *Sensors*, vol. 21, no. 10, p. 3540, May 2021, doi: 10.3390/s21103540.
51. W. Li, M. Ge, R. Jia, X. Zhao, H. Zhao, and C. Dong, "Design and Analysis Method of Piezoelectric Liquid Driving Device with Elastic External Displacement," *Micromachines (Basel)*, vol. 15, no. 4, p. 523, Apr. 2024, doi: 10.3390/mi15040523.
52. K. Uchino, "Piezoelectric ultrasonic motors: overview," *Smart Mater Struct*, vol. 7, no. 3, pp. 273–285, Jun. 1998, doi: 10.1088/0964-1726/7/3/002.
53. K. Uchino, S. Cagatay, B. Koc, S. Dong, P. Bouchilloux, and M. Strauss, "Micro Piezoelectric Ultrasonic Motors," *J Electroceram*, vol. 13, no. 1–3, pp. 393–401, Jul. 2004, doi: 10.1007/s10832-004-5131-x.
54. S. Ueha, Y. Hashimoto, M. Kuribayashi, and E. Mori, "Ultrasonic Power Measurement Using Standing Wave Ratio," *Jpn J Appl Phys*, vol. 24, no. S1, p. 169, Jan. 1985, doi: 10.7567/JJAPS.24S1.169.
55. Siyuan He, Weishan Chen, Xie Tao, and Zaili Chen, "Standing wave bi-directional linearly moving ultrasonic motor," *IEEE Trans Ultrason Ferroelectr Freq Control*, vol. 45, no. 5, pp. 1133–1139, Sep. 1998, doi: 10.1109/58.726435.
56. Y. Liu, S. Shi, C. Li, W. Chen, L. Wang, and J. Liu, "Development of a bi-directional standing wave linear piezoelectric actuator with four driving feet," *Ultrasonics*, vol. 84, pp. 81–86, Mar. 2018, doi: 10.1016/j.ultras.2017.10.017.
57. X. Dong, M. Hu, L. Jin, Z. Xu, and C. Jiang, "A standing wave ultrasonic stepping motor using open-loop control system," *Ultrasonics*, vol. 82, pp. 327–330, Jan. 2018, doi: 10.1016/j.ultras.2017.09.014.
58. X. Hou, H. P. Lee, C. J. Ong, and S. P. Lim, "Development and numerical characterization of a new standing wave ultrasonic motor operating in the 30–40kHz frequency range," *Ultrasonics*, vol. 53, no. 5, pp. 928–934, Jul. 2013, doi: 10.1016/j.ultras.2012.10.016.

59. L. Wang, C. Shu, Q. Zhang, and J. Jin, "A novel sandwich-type traveling wave piezoelectric tracked mobile system," *Ultrasonics*, vol. 75, pp. 28–35, Mar. 2017, doi: 10.1016/j.ultras.2016.11.006.
60. S. Kondo, H. Yamaura, D. Koyama, and K. Nakamura, "Traveling wave type ultrasonic linear motor using twin bending bars," *Phys Procedia*, vol. 3, no. 1, pp. 1053–1058, Jan. 2010, doi: 10.1016/j.phpro.2010.01.136.
61. D. Sun, S. Wang, S. Hata, J. Sakurai, and A. Shimokohbe, "Driving mechanism and experimental realization of a cylindrical ultrasonic linear microactuator," *Microelectron Eng*, vol. 86, no. 4–6, pp. 1262–1266, Apr. 2009, doi: 10.1016/j.mee.2008.12.087.
62. M. K. Kurosawa, "State-of-the-art surface acoustic wave linear motor and its future applications," *Ultrasonics*, vol. 38, no. 1–8, pp. 15–19, Mar. 2000, doi: 10.1016/S0041-624X(99)00087-6.
63. K. Asai, M. K. Kurosawa, and T. Higuchi, "Novel power circulation methods for a surface acoustic wave motor," in *1999 IEEE Ultrasonics Symposium. Proceedings. International Symposium (Cat. No.99CH37027)*, IEEE, 1999, pp. 667–670 vol.1. doi: 10.1109/ULTSYM.1999.849486.
64. M. Kurosawa, M. Takahashi, and T. Higuchi, "Ultrasonic linear motor using surface acoustic waves," *IEEE Trans Ultrason Ferroelectr Freq Control*, vol. 43, no. 5, pp. 901–906, Sep. 1996, doi: 10.1109/58.535493.
65. M. Kurosawa, M. Takahashi, and T. Higuchi, "Ultrasonic linear motor using surface acoustic waves," *IEEE Trans Ultrason Ferroelectr Freq Control*, vol. 43, no. 5, pp. 901–906, Sep. 1996, doi: 10.1109/58.535493.
66. M. Kuribayashi, S. Ueha, and E. Mori, "Excitation conditions of flexural traveling waves for a reversible ultrasonic linear motor," *J Acoust Soc Am*, vol. 77, no. 4, pp. 1431–1435, Apr. 1985, doi: 10.1121/1.392037.
67. M. Guo, S. Pan, J. Hu, C. Zhao, and S. Dong, "A small linear ultrasonic motor utilizing longitudinal and bending modes of a piezoelectric tube," *IEEE Trans Ultrason Ferroelectr Freq Control*, vol. 61, no. 4, pp. 705–709, Apr. 2014, doi: 10.1109/TUFFC.2014.2958.
68. K. Asumi, R. Fukunaga, T. Fujimura, and M. Kuribayashi Kurosawa, "High speed, high resolution ultrasonic linear motor using V-shape two bolt-clamped Langevin-type transducers," *Acoust Sci Technol*, vol. 30, no. 3, pp. 180–186, 2009, doi: 10.1250/ast.30.180.
69. M. Kuribayashi Kurosawa, O. Kodaira, Y. Tsuchitai, and T. Higuchi, "Transducer for high speed and large thrust ultrasonic linear motor using two sandwich-type vibrators," *IEEE Trans Ultrason Ferroelectr Freq Control*, vol. 45, no. 5, pp. 1188–1195, Sep. 1998, doi: 10.1109/58.726442.
70. A. Endo, N. Sasaki, and Y. Tomikawa, "Linear type ultrasonic motor using two-dimensionally positioned piezoelectric elements," *Ferroelectrics*, vol. 112, no. 1, pp. 165–170, Dec. 1990, doi: 10.1080/00150199008012792.
71. K. Uchino, K. Kato, and M. Tohda, "Ultrasonic linear motors using a multilayered piezoelectric actuator," *Ferroelectrics*, vol. 87, no. 1, pp. 331–334, Nov. 1988, doi: 10.1080/00150198808201395.
72. Z. Xue, K. T. Chau, W. Liu, and T. W. Ching, "Design, Analysis, and Implementation of Wireless Traveling-Wave Ultrasonic Motors," *IEEE Trans Power Electron*, vol. 39, no. 4, pp. 1–11, Apr. 2024, doi: 10.1109/TPEL.2024.3351142.
73. S. Guo, L. Wang, J. Jin, and Y. Yang, "A general structural design method, dynamics modeling and application study for built-in sandwich annular traveling wave piezoelectric transducers," *Mech Syst Signal Process*, vol. 199, p. 110476, Sep. 2023, doi: 10.1016/j.ymssp.2023.110476.
74. C. Jiang, Z. Zhao, D. Lu, Z. Xu, and L. Jin, "Contact analysis and performance evaluation of ring type traveling wave ultrasonic motors based on a surface contact model," *Ultrasonics*, vol. 127, p. 106851, Jan. 2023, doi: 10.1016/j.ultras.2022.106851.
75. T. Yang, B. Cao, Y. Chen, X. Li, J. He, and W. Su, "Optimization of three-dimensional traveling wave drive for a PZT thin-film micro-motor based on stiffness tuning of the supporting structure," *Ultrasonics*, vol. 134, p. 107066, Sep. 2023, doi: 10.1016/j.ultras.2023.107066.
76. Y. Zhang *et al.*, "Laser-induced microtextured stators coupling with flexible rotors for low-voltage driving rotational piezoelectric motors," *Chemical Engineering Journal*, vol. 467, p. 143361, Jul. 2023, doi: 10.1016/j.cej.2023.143361.
77. G. Wang *et al.*, "Improving output performance of ultrasonic motor by coating MoS2 on the stator," *Tribol Int*, vol. 186, p. 108608, Aug. 2023, doi: 10.1016/j.triboint.2023.108608.
78. K. Murai, D. Kong, H. Tamura, and M. Aoyagi, "Hollow cylindrical linear stator vibrator using a traveling wave of longitudinal axisymmetric vibration mode," *Ultrasonics*, vol. 129, p. 106910, Mar. 2023, doi: 10.1016/j.ultras.2022.106910.
79. C. Jiang, X. Wu, D. Lu, Z. Xu, and L. Jin, "Contact modeling and performance evaluation of ring type traveling wave ultrasonic motors considering stator teeth," *Ultrasonics*, vol. 117, p. 106518, Dec. 2021, doi: 10.1016/j.ultras.2021.106518.
80. X. Ma, J. Liu, J. Deng, Q. Liu, and Y. Liu, "A Rotary Traveling Wave Ultrasonic Motor With Four Groups of Nested PZT Ceramics: Design and Performance Evaluation," *IEEE Trans Ultrason Ferroelectr Freq Control*, vol. 67, no. 7, pp. 1462–1469, Jul. 2020, doi: 10.1109/TUFFC.2020.2972307.
81. N. Chen and D. Fan, "A teeth-discretized electromechanical model of a traveling-wave ultrasonic motor," *Mechanical Sciences*, vol. 11, no. 2, pp. 257–266, Jul. 2020, doi: 10.5194/ms-11-257-2020.

82. J. Li, S. Zeng, S. Liu, N. Zhou, and T. Qing, "Tribological properties of textured stator and PTFE-based material in travelling wave ultrasonic motors," *Friction*, vol. 8, no. 2, pp. 301–310, Apr. 2020, doi: 10.1007/s40544-018-0253-3.
83. S. Zeng, J. Li, N. Zhou, J. Zhang, A. Yu, and H. He, "Improving the wear resistance of PTFE-based friction material used in ultrasonic motors by laser surface texturing," *Tribol Int*, vol. 141, p. 105910, Jan. 2020, doi: 10.1016/j.triboint.2019.105910.
84. X. Liu, J. Song, H. Chen, G. Zhao, J. Qiu, and Q. Ding, "Enhanced transfer efficiency of ultrasonic motors with polyimide based frictional materials and surface texture," *Sens Actuators A Phys*, vol. 295, pp. 671–677, Aug. 2019, doi: 10.1016/j.sna.2019.06.033.
85. L. Kang *et al.*, "Design of precision driving control system for standing-wave ultrasonic motor," in *Eighth Symposium on Novel Photoelectronic Detection Technology and Applications*, S. Zhu, Q. Yu, J. Su, L. Chen, and J. Chu, Eds., SPIE, Mar. 2022, p. 592. doi: 10.1117/12.2626335.
86. Q. Pan, Y. Wang, A. Wan, C. Li, M. Zhao, and R. Li, "Development of a novel single-mode miniature standing wave ultrasonic motor," *Smart Mater Struct*, vol. 32, no. 12, p. 125015, Dec. 2023, doi: 10.1088/1361-665X/ad07a2.
87. Y. Deng, G. Zhao, X. Yi, and W. Xiao, "Contact modeling and input-voltage-region based parametric identification for speed control of a standing wave linear ultrasonic motor," *Sens Actuators A Phys*, vol. 295, pp. 456–468, Aug. 2019, doi: 10.1016/j.sna.2019.06.016.
88. Z. Chen, X. Li, P. Ci, G. Liu, and S. Dong, "A standing wave linear ultrasonic motor operating in in-plane expanding and bending modes," *Review of Scientific Instruments*, vol. 86, no. 3, Mar. 2015, doi: 10.1063/1.4914843.
89. Y. Shi and C. Zhao, "A new standing-wave-type linear ultrasonic motor based on in-plane modes," *Ultrasonics*, vol. 51, no. 4, pp. 397–404, May 2011, doi: 10.1016/j.ultras.2010.11.006.
90. Siyuan He, Weishan Chen, Xie Tao, and Zaili Chen, "Standing wave bi-directional linearly moving ultrasonic motor," *IEEE Trans Ultrason Ferroelectr Freq Control*, vol. 45, no. 5, pp. 1133–1139, Sep. 1998, doi: 10.1109/58.726435.
91. I. Grybas, R. Bansevicius, V. Jurenas, A. Bubulis, J. Janutenaite, and G. Kulvietis, "Ultrasonic standing waves-driven high resolution rotary table," *Precis Eng*, vol. 45, pp. 396–402, Jul. 2016, doi: 10.1016/j.precisioneng.2016.03.019.
92. M. Shafik and L. Makombe, "A Standing Wave Piezoelectric Ultrasonic Motor Using a Single Flexural Vibration Ring Transducer," *Applied Mechanics and Materials*, vol. 415, pp. 126–131, Sep. 2013, doi: 10.4028/www.scientific.net/AMM.415.126.
93. X. Lu, J. Hu, L. Yang, and C. Zhao, "A novel dual stator-ring rotary ultrasonic motor," *Sens Actuators A Phys*, vol. 189, pp. 504–511, Jan. 2013, doi: 10.1016/j.sna.2012.11.009.
94. X. Jin, Y. Zhang, H. Fu, J. Ji, X. Hua, and Y. Fu, "Low-voltage driving linear piezoelectric motors having textured sliders of surface multi-connected vesicle-like microarray," *Int J Mech Sci*, vol. 241, p. 107984, Mar. 2023, doi: 10.1016/j.ijmecsci.2022.107984.
95. Q. and P. Q. and Z. Y. and D. X. and F. H. and J. J. and W. P. L. and F. C. and L. J. and Y. Z. Peng, "Crocodile-Skin-Inspired Surface Microstructures for Friction Regulation of Piezoelectric Motors," *SSRN*, Oct. 2023.
96. Q. Peng *et al.*, "Mechanical Characteristics Regulation of V-Shaped Standing-Wave Ultrasonic Motors With Minimal Quantity Lubrication," *Tribology Transactions*, vol. 66, no. 2, pp. 222–237, Mar. 2023, doi: 10.1080/10402004.2023.2165465.
97. L. Zhou, Z. Yao, S. Dai, Y. He, and H. Xu, "Modeling and verification of life prediction of a V-shaped linear ultrasonic motor," *Review of Scientific Instruments*, vol. 92, no. 4, Apr. 2021, doi: 10.1063/5.0038358.
98. X. Li, Z. Yao, R. Li, and D. Wu, "Dynamics modeling and control of a V-shaped ultrasonic motor with two Langevin-type transducers," *Smart Mater Struct*, vol. 29, no. 2, p. 025018, Feb. 2020, doi: 10.1088/1361-665X/ab627a.
99. J. Wu *et al.*, "A two-DOF linear ultrasonic motor utilizing the actuating approach of longitudinal-traveling-wave/bending-standing-wave hybrid excitation," *Int J Mech Sci*, vol. 248, p. 108223, Jun. 2023, doi: 10.1016/j.ijmecsci.2023.108223.
100. H. Qu, C. Liu, L. Zhang, J. Qu, and B. Song, "A Longitudinal-Bending Hybrid Linear Ultrasonic Motor and Its Driving Characteristic," *Shock and Vibration*, vol. 2022, pp. 1–14, Jan. 2022, doi: 10.1155/2022/5701014.
101. Z. Ding, W. Wei, K. Wang, and Y. Liu, "An Ultrasonic Motor Using a Carbon-Fiber-Reinforced/Poly-Phenylene-Sulfide-Based Vibrator with Bending/Longitudinal Modes," *Micromachines* 2022, Vol. 13, Page 517, vol. 13, no. 4, p. 517, Mar. 2022, doi: 10.3390/M13040517.
102. D. Lu, Q. Lin, B. Chen, C. Jiang, and X. Hu, "A single-modal linear ultrasonic motor based on multi vibration modes of PZT ceramics," *Ultrasonics*, vol. 107, p. 106158, Sep. 2020, doi: 10.1016/j.ultras.2020.106158.
103. L. Yang, W. Ren, C. Ma, and L. Chen, "Mechanical simulation and contact analysis of the hybrid longitudinal-torsional ultrasonic motor," *Ultrasonics*, vol. 100, p. 105982, Jan. 2020, doi: 10.1016/j.ultras.2019.105982.

104. J. Deng, Y. Liu, J. Liu, D. Xu, and Y. Wang, "Development of a Planar Piezoelectric Actuator Using Bending-Bending Hybrid Transducers," *IEEE Transactions on Industrial Electronics*, vol. 66, no. 8, pp. 6141–6149, Aug. 2019, doi: 10.1109/TIE.2018.2873123.
105. Y. Liu, L. Wang, Z. Gu, Q. Quan, and J. Deng, "Development of a Two-Dimensional Linear Piezoelectric Stepping Platform Using Longitudinal-Bending Hybrid Actuators," *IEEE Transactions on Industrial Electronics*, vol. 66, no. 4, pp. 3030–3040, Apr. 2019, doi: 10.1109/TIE.2018.2842730.
106. J. Leng, L. Jin, Z. Xu, and X. Zhu, "Development of a 3-DOF Cylindrical Ultrasonic Motor Based on Non-Standard Modes," *Applied Sciences*, vol. 13, no. 18, p. 10096, Sep. 2023, doi: 10.3390/app131810096.
107. A. Mizuno, H. Kajiwara, H. Tamura, and M. Aoyagi, "Study on Multidegree-of-Freedom Ultrasonic Motor Using Vibration Mode Rotation of Metal Spherical Stator," *Actuators*, vol. 11, no. 1, p. 27, Jan. 2022, doi: 10.3390/act11010027.
108. Z. Li, Z. Guo, H. Han, Z. Su, and H. Sun, "Design and characteristic analysis of multi-degree-of-freedom ultrasonic motor based on spherical stator," *Review of Scientific Instruments*, vol. 93, no. 2, Feb. 2022, doi: 10.1063/5.0074049.
109. J. Leng, L. Jin, X. Dong, H. Zhang, C. Liu, and Z. Xu, "A multi-degree-of-freedom clamping type traveling-wave ultrasonic motor," *Ultrasonics*, vol. 119, p. 106621, Feb. 2022, doi: 10.1016/j.ultras.2021.106621.
110. S. Toyama, S. Hatae, and M. Nonaka, "Development of multi-degree of freedom spherical ultrasonic motor," in *Fifth International Conference on Advanced Robotics 'Robots in Unstructured Environments*, IEEE, 1991, pp. 55–60 vol.1. doi: 10.1109/ICAR.1991.240476.
111. S. Toyama, S. Sugitani, Zhang Guoqiang, Y. Miyatani, and K. Nakamura, "Multi degree of freedom spherical ultrasonic motor," in *Proceedings of 1995 IEEE International Conference on Robotics and Automation*, IEEE, pp. 2935–2940. doi: 10.1109/ROBOT.1995.525700.
112. R. Liu, L. Wang, J. Jin, and H. Zhao, "A Novel 2-Dof Ultrasonic Motor Design, Simulation, and Experimental Investigation," in *2022 16th Symposium on Piezoelectricity, Acoustic Waves, and Device Applications (SPAWDA)*, IEEE, Oct. 2022, pp. 77–81. doi: 10.1109/SPAWDA56268.2022.10045936.
113. Z. Huang, S. Shi, W. Chen, L. Wang, L. Wu, and Y. Liu, "Development of a novel spherical stator multi-DOF ultrasonic motor using in-plane non-axisymmetric mode," *Mech Syst Signal Process*, vol. 140, p. 106658, Jun. 2020, doi: 10.1016/j.ymssp.2020.106658.
114. Z. Li, Z. Wang, P. Guo, L. Zhao, and Q. Wang, "A ball-type multi-DOF ultrasonic motor with three embedded traveling wave stators," *Sens Actuators A Phys*, vol. 313, p. 112161, Oct. 2020, doi: 10.1016/j.sna.2020.112161.
115. V. Jūrėnas, G. Kazokaitis, and D. Mažeika, "Design of Unimorph Type 3DOF Ultrasonic Motor," *Applied Sciences*, vol. 10, no. 16, p. 5605, Aug. 2020, doi: 10.3390/app10165605.
116. X. Yang and W.-L. Zhu, "Design, Analysis, and Control of an XY Parallel Nanomanipulator With Multiple Actuation Modes," *IEEE Transactions on Industrial Electronics*, vol. 67, no. 9, pp. 7639–7648, Sep. 2020, doi: 10.1109/TIE.2019.2941137.
117. J. Deng, Y. Liu, S. Zhang, and J. Liu, "Modeling and experiments of a nano-positioning and high frequency scanning piezoelectric platform based on function module actuator," *Sci China Technol Sci*, vol. 63, no. 12, pp. 2541–2552, Dec. 2020, doi: 10.1007/s11431-020-1676-7.
118. D. Mazeika, S. Borodinas, P. Vasiljev, R. Bareikis, A. Struckas, and V. Jurenas, "2DOF LINEAR-ROTARY TYPE ULTRASONIC MOTOR."
119. Q. Chang, Y. Liu, J. Deng, S. Zhang, and W. Chen, "Design of a precise linear-rotary positioning stage for optical focusing based on the stick-slip mechanism," *Mech Syst Signal Process*, vol. 165, p. 108398, Feb. 2022, doi: 10.1016/j.ymssp.2021.108398.
120. Y. Sato, A. Kanada, and T. Mashimo, "Self-Sensing and Feedback Control for a Twin Coil Spring-Based Flexible Ultrasonic Motor," *IEEE Robot Autom Lett*, vol. 5, no. 4, pp. 5425–5431, Oct. 2020, doi: 10.1109/LRA.2020.3008118.
121. W. Wei *et al.*, "A linear ultrasonic motor driven by torsional/bending vibrations," *Sens Actuators A Phys*, vol. 357, p. 114404, Aug. 2023, doi: 10.1016/j.sna.2023.114404.
122. H.-K. Guo, Y.-H. Hsu, and C.-K. Lee, "Control of a multi-direction piezoelectric linear motor using a gyroscopic feedback control," in *Sensors and Smart Structures Technologies for Civil, Mechanical, and Aerospace Systems 2024*, M. P. Limongelli, C. T. Ng, and B. Glisic, Eds., SPIE, May 2024, p. 19. doi: 10.1117/12.3010023.
123. T. Yamabuchi and Y. Kagawa, "Numerical simulation of a piezoelectric ultrasonic motor and its characteristics," *J. Jpn. Soc. Simul. Technol*, vol. 8, no. 3, pp. 69–76, 1989.
124. T. Maeno, T. Tsukimoto, and A. Miyake, "Finite-element analysis of the rotor/stator contact in a ring-type ultrasonic motor," *IEEE Trans Ultrason Ferroelectr Freq Control*, vol. 39, no. 6, pp. 668–674, 1992.
125. J. W. Krome and J. Wallaschek, "Finite Element Models for the Piezoelectric Actuation in Ultrasonic Traveling Wave Motors," *J Intell Mater Syst Struct*, vol. 7, no. 2, pp. 157–161, Mar. 1996, doi: 10.1177/1045389X9600700206.
126. Z. Yin, C. Dai, Z. Cao, W. Li, Z. Chen, and C. Li, "Modal analysis and moving performance of a single-mode linear ultrasonic motor," *Ultrasonics*, vol. 108, p. 106216, Dec. 2020, doi: 10.1016/j.ultras.2020.106216.

127. W. Ren, M. Yang, L. Chen, C. Ma, and L. Yang, "Mechanical optimization of a novel hollow traveling wave rotary ultrasonic motor," *J Intell Mater Syst Struct*, vol. 31, no. 8, pp. 1091–1100, May 2020, doi: 10.1177/1045389X20910263.
128. L. Yang *et al.*, "Design and Dynamic Simulation of a Novel Traveling Wave Linear Ultrasonic Motor," *Micromachines (Basel)*, vol. 13, no. 4, p. 557, Mar. 2022, doi: 10.3390/mi13040557.
129. J. Li, F. Che, J. Deng, W. Chen, J. Liu, and Y. Liu, "A linear ultrasonic motor with a hollowed and symmetrical stator," *Int J Mech Sci*, vol. 262, p. 108718, Jan. 2024, doi: 10.1016/j.ijmecsci.2023.108718.
130. T. Kanda, A. Makino, T. Ono, K. Suzumori, T. Morita, and M. K. Kurosawa, "A micro ultrasonic motor using a micro-machined cylindrical bulk PZT transducer," *Sens Actuators A Phys*, vol. 127, no. 1, pp. 131–138, Feb. 2006, doi: 10.1016/j.sna.2005.10.056.
131. P. Marter, M. Khramova, F. Duvigneau, R. J. Wood, D. Juhre, and R. Orszulik, "Bidirectional motion of a planar fabricated piezoelectric motor based on unimorph arms," *Sens Actuators A Phys*, vol. 377, Oct. 2024, doi: 10.1016/j.sna.2024.115642.
132. T. Yang *et al.*, "A PZT Thin-Film Traveling-Wave Micro-Motor With Stator Teeth Based on MEMS Technology," *Journal of Microelectromechanical Systems*, vol. 33, no. 2, pp. 236–247, Apr. 2024, doi: 10.1109/JMEMS.2023.3348792.
133. W. Zhou *et al.*, "A Piezoelectric Microultrasonic Motor With High Q and Good Mode Match," *IEEE/ASME Transactions on Mechatronics*, vol. 26, no. 4, pp. 1773–1781, Aug. 2021, doi: 10.1109/TMECH.2021.3067774.
134. S. Cagatay, B. Koc, P. Moses, and K. Uchino, "A piezoelectric micromotor with a stator of $\varphi = 1.6\text{mm}$ and $l = 4\text{mm}$ using bulk PZT," *Japanese Journal of Applied Physics, Part 1: Regular Papers and Short Notes and Review Papers*, vol. 43, no. 4 A, pp. 1429–1433, 2004, doi: 10.1143/JJAP.43.1429.
135. K. Uchino, S. Cagatay, and B. Koc, "Ultrasonic Motors," 2003. [Online]. Available: <https://www.researchgate.net/publication/279377213>
136. S. Cagatay, B. Koc, and K. Uchino, "A 1.6-mm, Metal Tube Ultrasonic Motor," 2003.
137. K. Kikuchi, M. Hussain, and T. Mashimo, "Fabrication and characterization of a submillimeter-scale ultrasonic motor," *Sens Actuators A Phys*, vol. 360, p. 114524, Oct. 2023, doi: 10.1016/j.sna.2023.114524.
138. S. Izuhara and T. Mashimo, "Design and characterization of a thin linear ultrasonic motor for miniature focus systems," *Sens Actuators A Phys*, vol. 329, p. 112797, Oct. 2021, doi: 10.1016/j.sna.2021.112797.
139. B. Delibas and B. Koc, "Single crystal piezoelectric motor operating with both inertia and ultrasonic resonance drives," *Ultrasonics*, vol. 136, p. 107140, Jan. 2024, doi: 10.1016/j.ultras.2023.107140.
140. N. Chen, J. Zheng, X. Jiang, S. Fan, and D. Fan, "Analysis and control of micro-stepping characteristics of ultrasonic motor," *Frontiers of Mechanical Engineering*, vol. 15, no. 4, pp. 585–599, Dec. 2020, doi: 10.1007/s11465-019-0577-3.
141. Z. Li, Z. Wang, L. Zhao, and P. Guo, "Characteristic analysis and experimental study of spherical ultrasonic motor with multi-degree-of-freedom," *Journal of Applied Science and Engineering*, vol. 23, no. 4, pp. 619–626, Dec. 2020, doi: 10.6180/jase.202012_23(4).0006.
142. X. Li, Z. Wen, B. Jia, T. Cao, D. Yu, and D. Wu, "A Review of Application and Development Trends in Ultrasonic Motors," *ES Materials & Manufacturing*, 2020, doi: 10.30919/esmm5f933.
143. L. Zhang, H. Zheng, S. Huang, W. Zhang, F. Li, and D. Liu, "A life test of ultrasonic motors under different torque loads and the analysis of the characteristics of wearing surfaces," *Proceedings of the Institution of Mechanical Engineers, Part J: Journal of Engineering Tribology*, vol. 234, no. 5, pp. 770–777, May 2020, doi: 10.1177/1350650119871803.
144. "Ultrasonics: Fundamentals, Technologies, and Applications - Dale Ensminger, Leonard J. Bond - Google Books." Accessed: May 31, 2024. [Online]. Available: <https://books.google.com/books?hl=en&lr=&id=EVnqEAAQBAJ&oi=fnd&pg=PP1&dq=+ultrasonics+motors+in+Semiconductor+Manufacturing&ots=TIGXh-YtVV&sig=7PVusgeNkbYOJfIhcFwA8ANCvNU#v=onepage&q&f=false>
145. K. Guo, J. Lu, and H. Yang, "Simulation Analysis of a Sandwich Cantilever Ultrasonic Motor for a Dexterous Prosthetic Hand," *Micromachines* 2023, Vol. 14, Page 2150, vol. 14, no. 12, p. 2150, Nov. 2023, doi: 10.3390/Mi14122150.
146. K. Asumi, R. Fukunaga, T. Fujimura, and M. K. Kurosawa, "Miniaturization of a V-shape transducer ultrasonic motor," *Jpn J Appl Phys*, vol. 48, no. 7 PART 2, p. 07GM02, Jul. 2009, doi: 10.1143/JJAP.48.07GM02/XML.
147. T. Kimmel, S. Stall, D. Porada, C. Kunkel, and A. Kessler, "Comparison of ultrasonic devices for the pretreatment of textiles before washing and analysis of action," *J Eng Fiber Fabr*, vol. 18, Jan. 2023, doi: 10.1177/15589250231217086/ASSET/IMAGES/LARGE/10.1177_15589250231217086-FIG10.JPEG.
148. C. Dils, S. Hohner, and M. Schneider-Ramelow, "Use of Rotary Ultrasonic Plastic Welding as a Continuous Interconnection Technology for Large-Area e-Textiles," *Textiles* 2023, Vol. 3, Pages 66-87, vol. 3, no. 1, pp. 66–87, Jan. 2023, doi: 10.3390/TEXTILES3010006.

149. N. M. Zashchepkina, V. G. Zdorenko, N. R. Tierentyeva, O. M. Markina, M. O. Markin, and K. M. Bozhko, "Ultrasonic method of quality control for textile materials," *Archives of Materials Science and Engineering*, vol. Vol. 97, no. nr 1/2, pp. 39–49, 2019, doi: 10.5604/01.3001.0013.2867.
150. J. A. Gallego-Juarez, E. Riera, V. Acosta, G. Rodríguez, and A. Blanco, "Ultrasonic system for continuous washing of textiles in liquid layers," *Ultrason Sonochem*, vol. 17, no. 1, pp. 234–238, Jan. 2010, doi: 10.1016/J.ULTSONCH.2009.06.005.
151. K. Rapouch and Mrázek M, "Use of ultrasound for cleaning of components of historical vehicles in Technical Museum", doi: 10.2478/kom-2020-0012.
152. F. I. Alzarooni, A. K. Alkharji, A. A. Alsuwaidi, and E. R. Almajali, "Design and implementation of an automated dry solar-panel cleaning system," *2020 Advances in Science and Engineering Technology International Conferences, ASET 2020*, Feb. 2020, doi: 10.1109/ASET48392.2020.9118209.
153. T. Kimmel, C. Kunkel, M. Ait Sghir, and A. Kessler, "Potential of ultrasonics for energy saving in the household washing process," *Energy Effic*, vol. 16, no. 5, pp. 1–11, Jun. 2023, doi: 10.1007/S12053-023-10115-7/FIGURES/5.
154. J. Huang and D. Sun, "Performance Analysis of a Travelling-Wave Ultrasonic Motor under Impact Load," *Micromachines (Basel)*, vol. 11, no. 7, p. 689, Jul. 2020, doi: 10.3390/mi11070689.
155. X. Liu, G. Zhao, and J. Qiu, "Improving the performance of ultrasonic motors in low-pressure, variable-temperature environments," *Tribol Int*, vol. 160, p. 107000, Aug. 2021, doi: 10.1016/J.TRIBOINT.2021.107000.
156. E. T. K. Chiang, T. Urakubo, and T. Mashimo, "Lift Generation by a Miniature Piezoelectric Ultrasonic Motor-Driven Rotary-Wing for Pico Air Vehicles," *IEEE Access*, vol. 10, pp. 13210–13218, 2022, doi: 10.1109/ACCESS.2022.3146866.
157. J. Zhou *et al.*, "Development of a Δ -Type Mobile Robot Driven by Three Standing-Wave-Type Piezoelectric Ultrasonic Motors," *IEEE Robot Autom Lett*, vol. 5, no. 4, pp. 6717–6723, Oct. 2020, doi: 10.1109/LRA.2020.3018031.
158. Q. Lu, Z. Sun, J. Zhang, J. Zhang, J. Zheng, and F. Qian, "A Novel Remote-Controlled Vascular Interventional Robotic System Based on Hollow Ultrasonic Motor," *Micromachines (Basel)*, vol. 13, no. 3, p. 410, Mar. 2022, doi: 10.3390/mi13030410.
159. S. Izuhara and T. Mashimo, "Design and characterization of a thin linear ultrasonic motor for miniature focus systems," *Sens Actuators A Phys*, vol. 329, p. 112797, Oct. 2021, doi: 10.1016/j.sna.2021.112797.
160. K. Kikuchi, M. Hussain, and T. Mashimo, "Fabrication and characterization of a submillimeter-scale ultrasonic motor," *Sens Actuators A Phys*, vol. 360, Oct. 2023, doi: 10.1016/j.sna.2023.114524.
161. A. Antoniou *et al.*, "Robotic system for magnetic resonance guided focused ultrasound ablation of abdominal cancer," *The International Journal of Medical Robotics and Computer Assisted Surgery*, vol. 17, no. 5, p. e2299, Oct. 2021, doi: 10.1002/RCS.2299.
162. X. Bai, M. Hu, T. Gang, and Q. Rong, "A Submerged Optical Fiber Ultrasonic Sensor Using Matched Fiber Bragg Gratings," *Sensors*, vol. 18, no. 6, p. 1942, Jun. 2018, doi: 10.3390/s18061942.
163. J. Tian, X. Dong, S. Gao, and Y. Yao, "Multipoint fiber-optic laser-ultrasonic actuator based on fiber core-opened tapers," *Opt Express*, vol. 25, no. 24, p. 29737, Nov. 2017, doi: 10.1364/OE.25.029737.
164. M. Giannakou *et al.*, "Magnetic resonance image-guided focused ultrasound robotic system for transrectal prostate cancer therapy," *The International Journal of Medical Robotics and Computer Assisted Surgery*, vol. 17, no. 3, p. e2237, Jun. 2021, doi: 10.1002/RCS.2237.
165. C. Damianou, M. Giannakou, G. Menikou, and L. Ioannou, "Magnetic resonance imaging-guided focused ultrasound robotic system with the subject placed in the prone position," *Digit Med*, vol. 6, no. 1, pp. 24–31, Jan. 2020, doi: 10.4103/DIGM.DIGM_2_20.
166. A. Mustafa, T. Sasamura, and T. Morita, "Robust Speed Control of Ultrasonic Motors Based on Deep Reinforcement Learning of a Lyapunov Function," *IEEE Access*, vol. 10, pp. 46895–46910, 2022, doi: 10.1109/ACCESS.2022.3170995.
167. Y. J. Mon, "Vision Robot Path Control Based on Artificial Intelligence Image Classification and Sustainable Ultrasonic Signal Transformation Technology," *Sustainability 2022, Vol. 14, Page 5335*, vol. 14, no. 9, p. 5335, Apr. 2022, doi: 10.3390/SU14095335.
168. J. Sun, D. Zhou, Y. Liu, J. Deng, and S. Zhang, "Development of a Minimally Invasive Surgical Robot Using Self-Helix Twisted Artificial Muscles," *IEEE Transactions on Industrial Electronics*, vol. 71, no. 2, pp. 1779–1789, Feb. 2024, doi: 10.1109/TIE.2023.3257374.
169. J. Li, H. Liu, J. Li, Y. Yang, and S. Wang, "Piezoelectric transducer design for an ultrasonic scalpel with enhanced dexterity for minimally invasive surgical robots," <https://doi.org/10.1177/0954406219892750>, vol. 234, no. 7, pp. 1271–1285, Dec. 2019, doi: 10.1177/0954406219892750.
170. M. Pavone *et al.*, "Ultrasound-guided robotic surgical procedures: a systematic review," *Surg Endosc*, vol. 38, no. 5, pp. 2359–2370, May 2024, doi: 10.1007/s00464-024-10772-4.
171. R. Y. Hutama, M. M. Khalil, and T. Mashimo, "A Millimeter-Scale Rolling Microrobot Driven by a Micro-Geared Ultrasonic Motor," *IEEE Robot Autom Lett*, vol. 6, no. 4, pp. 8158–8164, Oct. 2021, doi: 10.1109/LRA.2021.3104227.

172. J. Li, Z. Sun, H. Yan, and J. Chen, "Design of a Magnetically Anchored Laparoscope Using Miniature Ultrasonic Motors," *Micromachines* 2022, Vol. 13, Page 855, vol. 13, no. 6, p. 855, May 2022, doi: 10.3390/MI13060855.
173. X. Li, T. Stritch, K. Manley, and M. Lucas, "Limits and Opportunities for Miniaturizing Ultrasonic Surgical Devices Based on a Langevin Transducer," *IEEE Trans Ultrason Ferroelectr Freq Control*, vol. 68, no. 7, pp. 2543–2553, Jul. 2021, doi: 10.1109/TUFFC.2021.3065207.
174. Q. Lu, Z. Sun, H. Yan, J. Zhang, J. Zhang, and J. Yang, "A novel laparoscopic surgical robot (LSR) based on double-leg ultrasonic motor (DUM)," *J Intell Mater Syst Struct*, vol. 34, no. 11, pp. 1276–1288, Jul. 2023, doi: 10.1177/1045389X221131806.
175. K. Fukushima *et al.*, "A pneumatic rotary actuator for forceps tip rotation," *Sens Actuators A Phys*, vol. 333, p. 113222, Jan. 2022, doi: 10.1016/j.sna.2021.113222.
176. Y. Qin, Y. Shi, L. Wang, H. Wang, and J. Han, "Design, Modeling and Optimization of a Magnetic Resonance Conditional 3-RRR Spherical Parallel Robot for Neurosurgery," *IEEE Trans Med Robot Bionics*, vol. 6, no. 2, pp. 556–566, May 2024, doi: 10.1109/TMRB.2024.3387114.
177. F. Ju *et al.*, "A Flexible Surgical Robot with Hemispherical Magnet Array Steering and Embedded Piezoelectric Beacon for Ultrasonic Position Sensing," *Advanced Intelligent Systems*, vol. 6, no. 3, Mar. 2024, doi: 10.1002/aisy.202300641.
178. S. Manjila, B. Rosa, K. Price, R. Manjila, M. Mencattelli, and P. E. Dupont, "Robotic Instruments Inside the MRI Bore: Key Concepts and Evolving Paradigms in Imaging-enhanced Cranial Neurosurgery," *World Neurosurg*, vol. 176, pp. 127–139, Aug. 2023, doi: 10.1016/j.wneu.2023.01.025.
179. B. Li, L. Yuan, C. Wang, and Y. Guo, "Structural design and analysis of pneumatic prostate seed implantation robot applied in magnetic resonance imaging environment," *The International Journal of Medical Robotics and Computer Assisted Surgery*, vol. 18, no. 6, Dec. 2022, doi: 10.1002/rcs.2457.
180. M. Li, "Design and stability analysis of a nonlinear controller for MRI-compatible pneumatic motors," *Proc Inst Mech Eng C J Mech Eng Sci*, vol. 238, no. 1, pp. 3–17, Jan. 2024, doi: 10.1177/09544062231171994.
181. A. L. Gunderman, M. Azizkhani, S. Sengupta, K. Cleary, and Y. Chen, "Modeling and Control of an MR-Safe Pneumatic Radial Inflow Motor and Encoder (PRIME)," *IEEE/ASME Transactions on Mechatronics*, pp. 1–12, 2023, doi: 10.1109/TMECH.2023.3329296.
182. X. T. Wankhede SP, "The Roles of Piezoelectric Ultrasonic Motors in Industry 4.0 Era: Opportunities & Challenges..," in *Piezoelectric Actuators-Principles, Design, Experiments and Applications*, Hu Huang and Jianping Li, Eds., IntechOpen, 2021, ch. 8.
183. X. Li *et al.*, "A Design Method of Traveling Wave Rotary Ultrasonic Motors Driving Circuit under High Voltage Using Single-Sided Hertzian Contact Forced Oscillator Model," *Micromachines (Basel)*, vol. 14, no. 1, p. 64, Dec. 2022, doi: 10.3390/mi14010064.
184. C.-P. Lee, M.-C. Tsai, and Y.-K. Fuh, "Tiny Piezoelectric Multi-Layered Actuators with Application in a Compact Camera Module—Design, Fabrication, Assembling and Testing Issues," *Micromachines (Basel)*, vol. 13, no. 12, p. 2126, Dec. 2022, doi: 10.3390/mi13122126.
185. X. Xin, X. Gao, J. Wu, Z. Li, Z. Chu, and S. Dong, "A ring-shaped, linear piezoelectric ultrasonic motor operating in E01 mode," *Appl Phys Lett*, vol. 116, no. 15, Apr. 2020, doi: 10.1063/5.0006524.
186. R. Niu, H. Zhu, and C. Zhao, "A four-legged linear ultrasonic motor: Design and experiments," *Review of Scientific Instruments*, vol. 91, no. 7, Jul. 2020, doi: 10.1063/1.5114787.
187. X. Ma *et al.*, "A novel rotary ultrasonic motor based on multiple Langevin transducers: design, simulation, and experimental investigation," *Smart Mater Struct*, vol. 33, no. 5, p. 055001, May 2024, doi: 10.1088/1361-665X/ad37b4.
188. X. Ma, J. Liu, J. Deng, Q. Liu, and Y. Liu, "A Rotary Traveling Wave Ultrasonic Motor With Four Groups of Nested PZT Ceramics: Design and Performance Evaluation," *IEEE Trans Ultrason Ferroelectr Freq Control*, vol. 67, no. 7, pp. 1462–1469, Jul. 2020, doi: 10.1109/TUFFC.2020.2972307.
189. S. Guo, L. Wang, J. Jin, and Y. Yang, "A general structural design method, dynamics modeling and application study for built-in sandwich annular traveling wave piezoelectric transducers," *Mech Syst Signal Process*, vol. 199, p. 110476, Sep. 2023, doi: 10.1016/j.ymssp.2023.110476.
190. Z. Xue, K. T. Chau, W. Liu, and T. W. Ching, "Design, Analysis, and Implementation of Wireless Traveling-Wave Ultrasonic Motors," *IEEE Trans Power Electron*, vol. 39, no. 4, pp. 4601–4611, Apr. 2024, doi: 10.1109/TPEL.2024.3351142.
191. Y. Zhang *et al.*, "Laser-induced microtextured stators coupling with flexible rotors for low-voltage driving rotational piezoelectric motors," *Chemical Engineering Journal*, vol. 467, p. 143361, Jul. 2023, doi: 10.1016/j.cej.2023.143361.
192. L. Yang *et al.*, "A novel traveling wave rotary ultrasonic motor with piezoelectric backup function," *J Intell Mater Syst Struct*, vol. 34, no. 20, pp. 2414–2427, Dec. 2023, doi: 10.1177/1045389X231187484.
193. Z. Wen, X. Li, T. Cao, B. Wang, R. Liu, and D. Wu, "A Low-Voltage Cylindrical Traveling Wave Ultrasonic Motor Incorporating Multilayered Piezoelectric Ceramics," *IEEE Trans Ultrason Ferroelectr Freq Control*, vol. 69, no. 6, pp. 2129–2136, Jun. 2022, doi: 10.1109/TUFFC.2022.3164940.

194. Y. Liu, Y. Xiong, L. Hua, L. Yang, and W. Zeng, "Mechanical characteristic analysis of a separable stator fabricated by fine-blanking process with numerical and experimental methods," *The International Journal of Advanced Manufacturing Technology*, vol. 112, no. 9–10, pp. 2435–2445, Feb. 2021, doi: 10.1007/s00170-020-06414-3.
195. T.-B. Xu, "Review on PMN-PT Relaxor Piezoelectric Single Crystal materials for cryogenic actuators," in *AIAA SCITECH 2022 Forum*, Reston, Virginia: American Institute of Aeronautics and Astronautics, Jan. 2022. doi: 10.2514/6.2022-2240.
196. T.-B. Xu, L. Tolliver, X. Jiang, and J. Su, "A single crystal lead magnesium niobate-lead titanate multilayer-stacked cryogenic flextensional actuator," *Appl Phys Lett*, vol. 102, no. 4, Jan. 2013, doi: 10.1063/1.4790142.

Disclaimer/Publisher's Note: The statements, opinions and data contained in all publications are solely those of the individual author(s) and contributor(s) and not of MDPI and/or the editor(s). MDPI and/or the editor(s) disclaim responsibility for any injury to people or property resulting from any ideas, methods, instructions or products referred to in the content.